



HAL
open science

Genetically-achieved disturbances to the expression levels of TNFSF11 receptors modulate the effects of zoledronic acid on growing mouse skeletons

Jorge William Vargas-Franco, Beatriz Castaneda, Andrea Gama, Christopher Mueller, Dominique Heymann, Françoise Rédini, Frederic Lezot

► To cite this version:

Jorge William Vargas-Franco, Beatriz Castaneda, Andrea Gama, Christopher Mueller, Dominique Heymann, et al.. Genetically-achieved disturbances to the expression levels of TNFSF11 receptors modulate the effects of zoledronic acid on growing mouse skeletons. *Biochemical Pharmacology*, 2019, 168, pp.133-148. 10.1016/j.bcp.2019.06.027 . hal-02884673

HAL Id: hal-02884673

<https://hal.science/hal-02884673>

Submitted on 25 Oct 2021

HAL is a multi-disciplinary open access archive for the deposit and dissemination of scientific research documents, whether they are published or not. The documents may come from teaching and research institutions in France or abroad, or from public or private research centers.

L'archive ouverte pluridisciplinaire **HAL**, est destinée au dépôt et à la diffusion de documents scientifiques de niveau recherche, publiés ou non, émanant des établissements d'enseignement et de recherche français ou étrangers, des laboratoires publics ou privés.



Distributed under a Creative Commons Attribution - NonCommercial 4.0 International License

Genetically-achieved disturbances to the expression levels of TNFSF11 receptors modulate the effects of zoledronic acid on growing mouse skeletons.

Jorge William Vargas-Franco^{1,2}, Beatriz Castaneda³, Andrea Gama^{4,5,6}, Christopher Mueller⁷,
Dominique Heymann^{8,9}, Françoise Rédini¹, Frédéric Lézot¹ *

1. INSERM, UMR-1238, Equipe 1, Faculté de Médecine, Université de Nantes, Nantes, F-44035, France.
2. Department of Basic Studies, Faculty of Odontology, University of Antioquia, Medellin, Colombia.
3. Service d'Odontologie-Stomatologie, Hôpital Pitié-Salpêtrière, AP-HP, Paris, F-75013, France.
4. INSERM, UMR-1138, Equipe 5, Centre de Recherche des Cordeliers, Paris, F-75006, France.
5. Odontology Center of District Federal Military Police, Brasília, Brazil.
6. Oral Histopathology Laboratory, Health Sciences Faculty, University of Brasília, Brasília, Brazil.
7. CNRS, UPR 9021, Institut de Biologie Moléculaire et Cellulaire (IBMC), Laboratoire Immunologie et Chimie Thérapeutiques, Université de Strasbourg, Strasbourg, F-67084 France.
8. INSERM, LEA Sarcoma Research Unit, University of Sheffield, Department of Oncology and Human Metabolism, Medical School, Sheffield, S10 2RX, UK.

9. INSERM, UMR 1232, LabCT, Université de Nantes, Université d'Angers, Institut de Cancérologie de l'Ouest, site René Gauducheau, Saint-Herblain, F-44805, France.

**Corresponding author:*

Dr Frédéric Lézot

INSERM UMR1238 - Faculté de Médecine de Nantes

1, rue Gaston Veil, F44035, Nantes, France

Email: Frederic.lezot@univ-nantes.fr; Tel: 00 33 240 412 846; Fax: 00 33 240 412 870

Running title: RANKL signaling and effects of zoledronic acid during growth

Abstract

Zoledronic acid (ZOL), a nitrogen bisphosphonate (N-BP), is currently used to treat and control pediatric osteolytic diseases. Variations in the intensity of the effects and side effects of N-BPs have been reported with no clear explanations regarding their origins. We wonder if such variations could be associated with different levels of RANKL signaling activity in growing bone during and after the treatment with N-BPs. To answer this question, ZOL was injected into neonate C57BL/6J mice with different genetically-determined RANKL signaling activity levels (*Opg*^{+/+}*Rank*^{Tg-}, *Opg*^{+/+}*Rank*^{Tg+}, *Opg*^{+/-}*Rank*^{Tg-}, *Opg*^{+/-}*Rank*^{Tg+}, *Opg*^{-/-}*Rank*^{Tg-} and *Opg*^{-/-}*Rank*^{Tg+} mice) following a protocol (4 injections from post-natal day 1 to 7 at the dose of 50 µg/kg) that mimics those used in onco-pediatric patients. At the end of pediatric growth (1 and half months) and at an adult age (10 months), the bone morphometric and mineral parameters were measured using µCT in the tibia and skull for the different mice. A histologic analysis of the dental and periodontal tissues was also performed. At the end of pediatric growth, a delay in long bone and skull bone growth, a blockage of tooth eruption, some molar root alterations and a neoplasia-like structure associated with incisor development were found. Interestingly, the magnitude of these side effects was reduced by *Opg* deficiency (*Opg*^{-/-}) but increased by *Rank* overexpression (*Rank*^{Tg}). Analysis of the skeletal phenotype at ten months confirmed respectively the beneficial and harmful effects of *Opg* deficiency and *Rank* overexpression.

These results validated the hypothesis that the RANKL signaling activity level in the bone microenvironment is implicated in the modulation of the response to ZOL. Further studies will be necessary to understand the underlying molecular mechanisms, which will help decipher the variability in the effects of N-BPs reported in the human population.

Keywords: Zoledronic acid; RANKL/RANK/OPG; Long bone; Craniofacial bone; Growth; Tooth.

Significant statements

The present study establishes that in mice the RANKL signaling activity level is a major modulator of the effects and side-effects of bisphosphonates on the individual skeleton during growth. However, the modulatory actions are dependent on the ways in which this level of activity is increased. A decrease in OPG expression is beneficial to the skeletal phenotype observed at the end of growth, while RANK overexpression deteriorates it. Far removed from pediatric treatment, in adults, the skeletal phenotypes initially observed at the end of growth for the different levels of RANKL signaling activity were maintained, although significant improvement was associated only with reductions in OPG expression.

1. Introduction

Zoledronic acid (ZOL), one of the most potent amino-bisphosphonates (N-BPs), is currently used in clinical practice to control pediatric osteolytic diseases regardless of their genetic, endocrine, inflammatory or oncogenic origins (for review [1]). Despite its proven efficacy in the treatment of these systemic or local diseases, several side-effects on axial, appendicular and craniofacial growing skeletons have been reported in either preclinical or clinical studies [2–8]. Some of these side-effects were presented as reversible after the end of treatment, for instance the arrest of long bone growth, others as definitive, for instance the failure of dental eruption (for review [1]). Today, these side-effects are presented as direct consequences of the loss of osteoclast function, inducing an osteopetrotic-like phenotype. However, this presentation does not explain the significant variations in the penetrance of these side-effects in pediatric patients, as well as in mouse pups from different strains treated with ZOL [4,9]. Different causes have been suggested for such variations in the penetrance of N-BP side-effects. This included on the one hand drug-related causes, such as the pharmacological properties of the drug (pharmacokinetics and pharmacodynamics), doses, duration of the therapy, drug interactions and pharmacogenetics, and on the other, host-related causes such as expression levels in the bone cells of genetic and epigenetic factors, and the composition in the cytokines/chemokines in the bone microenvironment [1,4,9–13]. Surprisingly, none of these causes have been analyzed in depth so far. The main objective of the present manuscript was thus to investigate in depth one potential host-related cause, which is the level of activity of TNFSF11 (currently named RANKL for receptor activator of nuclear factor kappa B ligand) signaling. Two transgenic mouse models of genetically-achieved

disturbances to this signaling, plus an already-established and validated protocol of ZOL pediatric treatment inducing craniofacial and appendicular skeleton side-effects [4,9] were used. This signaling was chosen in relation to its importance during growth in the osteoclastogenesis in either the axial, appendicular or craniofacial skeletons [14–16], in the immune/inflammatory response [14,15] and in the cell-to-cell communications necessary for the development of many organs, including all skeleton components [17–19]. The two mouse models corresponded to an over-expression of TNFRSF11a (also called RANK) driven in the monocyte/macrophage lineage by the *Mrp8* (myeloid related protein 8) promoter and a global invalidation of TNFRSF11b (also called OPG, for osteoprotegerine). These two proteins have opposing functions regarding RANKL signaling. RANK is a transmembrane receptor expressed at the surface of RANKL signaling target-cells such as osteoclasts, but also dendritic cells and endothelial cells [20–22], while OPG is a secreted protein that binds to RANKL and inhibits its signaling through RANK [20–22]. Consequently, both transgenic mouse models correspond to over-activation of RANKL signaling, achieved by two complementary approaches that make possible combinations for obtaining a series of mice with graded levels of RANKL signaling activation.

Few studies have analyzed the impact of N-BPs on the relative expressions of the elements of the RANK\RANKL\OPG triad [23,24], whereas the consequences of disturbances to the expression levels of RANKL receptors on the effects and side-effects of N-BPs on skeletons have never been evaluated. This is all the more surprising given that the osteolytic diseases associated with a gain in RANK function (namely Expansile Skeletal Hyperphosphatasia (ESH), Familial Expansile Osteolysis (FEO) and Paget Disease of Bone 2, early-onset

(PDB2)) [25], or OPG loss of function (namely Paget Disease of Bone 5, juvenile-onset (PDB5)) [26,27] are currently treated with N-BPs [27,28].

The present study aims to establish, using combinations of two transgenic mouse models, the consequences of disturbances to the expression levels of RANKL receptors on the effects and side-effects of neonatal ZOL treatment on both the appendicular and craniofacial skeletons, at the end of pediatric growth (one-month post-treatment) and in the longer-term (at ten months of age).

2. Materials and Methods

2.1. Animals

The mice were housed under pathogen-free conditions at the Experimental Therapy Unit (Faculty of Medicine, Nantes, France) in accordance with the institutional European guidelines (EU directive 2010/63/EU). All protocols applied in the present study were first validated by the French ethical committee of the “Pays de la Loire” (CEEA-PdL-06) and authorized by the French ministry of agriculture and fisheries (authorization # 11208-2017083115577055). The mice were handled and sacrificed by authorized investigators in strict respect of these protocols.

Two transgenic mouse models on a C57BL/6J background were used in the experimentations corresponding to the purchased *Tnfrsf-11b* (osteoprotegerin: *Opg*) knock-out model (Strain B6.129S4-Tnfrsf11b^{tm1Eac}/J, Stock 010672, The Jackson Laboratory, Bar Harbor, ME, USA) and the *Tnfrsf-11a* (receptor activator of nuclear factor kappa B: *Rank*) over-expression model we created previously [29]. These two models were mated to obtain all possible combinations (*Opg*^{+/+}*Rank*^{Tg-}, *Opg*^{+/+}*Rank*^{Tg+}, *Opg*^{+/-}*Rank*^{Tg-}, *Opg*^{+/-}*Rank*^{Tg+}, *Opg*^{-/-}*Rank*^{Tg-} and *Opg*^{-/-}*Rank*^{Tg+}). The genotypes were determined by PCR, using genomic DNA extracted from the tail of each mouse, as previously described [16].

2.2. Zoledronic acid treatment

The protocol of zoledronic acid (ZOL) administration was designed according to the pharmacokinetics data of ZOL, and mimicking the clinical protocol administered in pediatric patients with primary bone tumors as previously described [4,9]. Briefly, mouse pups were

randomly divided into treated and non-treated groups. In the treated group, each pup received 4 subcutaneous injections of 50 µg/kg of ZOL (Zometa®, Novartis Pharmaceuticals Corporation, Basel, Switzerland) on days 1, 3, 5 and 7 after birth (Fig. 1). In the non-treated group, each pup received 4 injections of sterile normal saline solution. In order to analyze the consequences of the treatment with ZOL at the end of growth, the mice were sacrificed at one and a half months. In order to analyze the long-term consequences of treatment with ZOL during growth, a group of twelve mice (two for each genotype) were maintained and followed until ten months of age.

2.3. Micro-CT analysis

A Skyscan 1076 micro-CT scanner (Skyscan, Kontich, Belgium) was used to analyze on the one hand the morphometric and mineral parameters of representative bones of appendicular and craniofacial skeletons (tibia, plus maxillary, basal and alveolar bones), and on the other the eruption status of molars and incisors.

All tibias and heads were scanned using the same parameters (pixel size 9µm, 50kV, 0.5mm Aluminum filter, 20 minutes of scanning). The reconstruction was carried out using NRecon, and the analyses were performed using CTAn, CTVox and DataViewer software (Skyscan). The different measurements were made using IMAGE-J software (National Institutes of Health, Bethesda, MD, USA). In this way, the acquisition of the image in CTVox was systematically calibrated with a phantom of 5mm (known size) and all measurements were finally sized using the analysis scale in the IMAGE-J software.

In order to analyze the effects of ZOL on growing appendicular skeletons, the right tibia was measured in all mice. For vertical growth, the longitudinal distance was seized. Concerning

axial growth, the external and internal diameters were measured and the difference between the measurements made it possible to determine cortical thickness. The marks of reference used for the tibia measurements are shown in Figure 2A.

In order to analyze the effects of ZOL on growing craniofacial skeletons, measurements were made using the method proposed by Vora et al. [30] and Simon et al. [31]. Eight measurements regarding the sagittal, vertical and transversal planes of craniofacial growth were made (Fig. 1A). The marks of reference used to perform these craniofacial measurements are presented in Figure 2A.

In order to obtain the bone mineral parameters, more specifically tissue mineral density (TMD) for cortical bone and the percentage of bone volume (BV/TV), the trabecula number (Tb.N) and trabecula thickness (Tb.Th) for trabecular, basal and alveolar bones, a sample volume of 2.0 mm in length, and measuring 1.1 mm x 1.1 mm in surface width was sectioned using the Data Viewer software, and analyzed using the CTAn software. The different points chosen for the analysis are presented in Figure 2B.

In order to facilitate identification of the changes in the different structures, a “color density range” was used in the CTAn software that made it possible to adjust the correspondence of color and brightness values using image gray scales. For the tibia and head images, brightness level 39 and contrast level 45 from the color density range of the CTAn software were used systematically.

2.4. Histology

Heads and tibias were collected from euthanized mice and were fixed in 4% buffered paraformaldehyde (Sigma-Aldrich, Saint-Quentin Fallavier, France). The samples were

decalcified in a buffered pH 7.4 solution containing 4.13% EDTA (Sigma-Aldrich) and 0.2% paraformaldehyde over 4 days in KOS sw10 (Milestone, Sorisole, Italy). All the samples were then dehydrated and embedded in paraffin according to the conventional methods. The samples were sectioned (3 μm -thick sections) and then stained with Masson's trichrome to analyze the morphology, or with tartrate-resistant acid phosphatase (TRAP) to identify multinucleated osteoclast cells as previously described [4]. Histological images were acquired using a Nano-Zoomer 2.0-RS slide scanner (Hamamatsu Photonics, Hamamatsu city, Japan) before being visualized and analyzed using Nano-Zoomer software.

2.5. Statistical analyses

All the measurements were analyzed using Prism (6.01) software (GraphPad Software, La Jolla, CA, USA). To determine the normality of the data, a Brown-Forsythe test was carried out, considering significantly standard deviations ($p < 0.05$). A one-way ANOVA followed by a Tukey post-test to compare all groups was performed to evidence statistically significant differences $p < 0.05$ (*), $p < 0.01$ (**); $p < 0.001$ (***) and $p < 0.0001$ (****).

3. Results

3.1. Appendicular skeletons of transgenic mice, with genetically-induced variations in OPG and RANK expression levels, were differentially affected at the end of growth following treatment with ZOL.

Bone morphometric (Fig. 3) and mineral parameters (Fig. 4) were measured at the end of growth (one and half months) on micro-CT scans of tibias obtained from mice from the different genotypes of either treated or non-treated groups. Regarding the morphometric parameters, the analysis of mice in the different genotypes without treatment (Fig. 3) did not reveal any significant difference in either vertical or axial growth (mean global length: 12.31 ± 1.04 ; mean global external diameter: 0.86 ± 0.09 ; mean global internal diameter: 0.58 ± 0.06 and mean global thickness: 0.14 ± 0.03). However, comparison of treated and non-treated mice from the same genotype revealed a significant reduction in all morphometric parameters except bone thickness in treated mice from the *Opg^{+/+}\Rank^{Tg-}*, *Opg^{+/-}\Rank^{Tg-}* and *Opg^{+/-}\Rank^{Tg+}* genotypes (Fig. 3). On the contrary, no such reduction was observed (Fig. 3) regardless of the parameter considered for the *Opg^{-/-}\Rank^{Tg-}* mice (for instance mean length 11.71 ± 0.90 for treated vs 11.48 ± 1.03) and *Opg^{-/-}\Rank^{Tg+}* mice (for instance mean length 11.82 ± 1.20 for treated vs 11.08 ± 1.90).

Regarding bone mineral parameters, in the absence of treatment, no significant difference was observed between the different genotypes (Fig. 4), although the TMD appeared slightly inferior in *Opg^{-/-}* (*RANK^{Tg-}* and *RANK^{Tg+}*) mice compared to mice from all other genotypes (mean 3.6 ± 0.4 vs 4.4 ± 0.3). In the treated group, TMD did not appear to be significantly

affected compared to the non-treated group, with respect to the genotypes, except in *Opg*^{-/-} \ *Rank*^{Tg+}, while all the other parameters, which had a value of zero in the non-treated group, appeared increased (Fig. 4). Interestingly, the observed values of these parameters were different with respect to the genotypes. Considering only *Opg* status, a relationship was observed between the values of the parameters and the allelic reductions, with *Opg*^{-/-} evidencing the lower parameters and *Opg*^{+/+} the higher (Fig.4). With regard to *Rank* status, genetically-achieved over-expression induced very significant elevations in all the parameters independently of *Opg* status (Fig. 4), except Tb.Th in *Opg*^{-/-} \ *Rank*^{Tg+}

3.2. Craniofacial skeletons of transgenic mice, with genetically-induced variations in OPG and RANK expression levels, were differentially affected at the end of growth following treatment with ZOL.

The craniofacial morphometric parameters and mineral parameters of maxillary basal and alveolar bones were measured at the end of growth (one and half months) on the micro-CT scans of heads obtained from mice from the different genotypes, treated or not with ZOL.

Regarding the morphometric parameters, analysis of the mice from the different genotypes from the non-treated group (Fig. 5) did not reveal any significant difference, with the exception of facial height, which appeared higher in the *Opg*^{-/-} mice (Fig. 5E). Interestingly, comparison of treated and non-treated mice from the same genotype revealed two different situations. First, for *Opg*^{+/+} \ *Rank*^{Tg-}, *Opg*^{+/-} \ *Rank*^{Tg-} and *Opg*^{+/+} \ *Rank*^{Tg+} mice, total skull length, cranial vault length, facial region length, and the upper and lower maxillary were significantly reduced in the treated group (Fig. 5 A, B, C, F and G), whereas the middle cranial vault, facial height

and cranial vault width were not affected (Fig. 5 D, E and H). Secondly, in *Opg^{-/-}Rank^{Tg-}* and *Opg^{-/-}Rank^{Tg+}* mice, none of the parameters were significantly affected by treatment with ZOL (Fig. 5).

For the bone mineral parameters, analysis of the different genotypes of the non-treated group (Fig. 6) revealed that basal and alveolar bones were not similarly modulated regarding BV/TV and Tb.Th, while they were close concerning the Tb.N. Effectively, the Tb.N in both bones was significantly lower only in *Opg^{-/-}Rank^{Tg-}* mice (Fig. 6C and D). For the other two parameters, alveolar bone appeared more affected than basal bone. Regardless, BV/TV appeared to decrease gradually and significantly compared to the *Opg^{+/+}Rank^{Tg-}* from the *Opg^{+/-}Rank^{Tg-}* to the *Opg^{-/-}Rank^{Tg+}* genotypes (Fig. 6A and B). For Tb.Th, a similarly graded decrease was observed for alveolar bone (Fig. 6E), while for basal bone this parameter was significantly decreased solely for the *Opg^{-/-}Rank^{Tg-}* mice (Fig. 6F).

Due to defective inter-radicular alveolar bone formation associated with blocked eruption and root elongation following ZOL treatment, measurements of bone mineral parameters were only possible for the basal bone in the treated group. Interestingly, the BV/TV and Tb.N increased significantly in the treated group, compared to the non-treated group, regardless of genotype (Fig. 6B and D), with very close values in all treated mice. Surprisingly, the Tb.Th was also significantly increased by the treatment, except in mice over-expressing *Rank* with however a noticeable tendency for increase (Fig. 6F).

Teeth are important elements in the craniofacial skeleton whose histogenesis/organogenesis is known to be sensitive to treatment with ZOL. More specifically, the eruption and root elongation processes have been shown to be disturbed by treatment with ZOL in C57BL/6J wild-type mice. In order to determine the consequences of OPG and RANK expression levels

on the severity of these disturbances, both processes were analyzed comparatively in mice with different genotypes. For the eruption process, micro-CT scans of heads were used (Fig. 7) to determine the eruption status in a three-step classification corresponding to fully-erupted (yellow), partially-erupted (clear blue) and not erupted (dark blue) teeth. For root elongation, histology was used, focusing on the first mandibular molars (Fig. 8).

In the absence of treatment, regardless of the genotypes considered, normal eruption was observed for either incisors or molars, and the dental structures revealed normal development (Fig. 7A and 8). The main specific feature observed in these untreated mice concerned the *Opg*^{-/-} mice (*Rank*^{Tg-} or *Rank*^{Tg+}), where small root resorption lacunas associated with the presence of numerous TRAP positive cells was observed (Fig. 8). A reduced diameter of the root was also present in the *RANK*^{Tg+} mice (visible, for instance, in Fig. 7A for *Opg*^{-/-}*Rank*^{Tg+} compared to *Opg*^{-/-}*Rank*^{Tg-}).

In the treated group, the dental phenotype was affected in all mice, although the proportions differed in relation to the genotypes (Fig. 7 and 8). Alterations to the eruption of the incisors (upper and lower) and first molars (upper and lower) were observed in all genotypes, but with a globally-graded decrease in penetrance from the *Opg*^{+/+}*Rank*^{Tg-} to the *Opg*^{-/-}*Rank*^{Tg+} mice (Fig. 7B). Interestingly, all teeth were not affected in the same way in each mouse, regardless of the genotype. For the eruption of the first molars, the most affected was the upper molar, 100% in *Opg*^{+/+}*Rank*^{Tg-}, *Opg*^{+/-}*Rank*^{Tg-} and *Opg*^{+/-}*Rank*^{Tg+} mice, while the lower molar was affected in around 80% in these mice (Fig. 7B). For the eruption of the incisors, a similar response was reported for these mice for the upper incisor (more than 80%) whereas lower incisor eruption was partially preserved (less than 40% affected). For *Opg*^{-/-} mice, eruption of the first molars and incisors was clearly less affected, with a maximum of 60% for the first

upper molar in *Opg^{-/-}Rank^{Tg-}* (impacted 40%, partial erupted 20%) and a minimum of 0% for the lower incisor in both *Opg^{-/-}Rank^{Tg-}* and *Opg^{-/-}Rank^{Tg+}* mice (Fig. 7B). It is important to emphasize that the eruption of the second and the third molars was unaffected regardless of the genotype considered (Fig. 7A).

For the histology of the mandibular first molar root, treatment with ZOL induced a blockage of the root elongation correlated to defective eruption regardless of the genotype considered (Fig. 8). On the contrary, when tooth eruption was effective (mainly in *Opg^{-/-}* mice, regardless of *Rank^{Tg}* status) close-to-normal root elongation was observed with surprisingly no visible root resorption lacunas compared to what could be seen in untreated *Opg^{-/-}* mice (Fig. 8). Interestingly, a graded increase in the numbers of TRAP positive cells (black arrow-heads) was observed at the alveolar bone surface from *Opg^{+/+}Rank^{Tg-}* to *Opg^{-/-}Rank^{Tg+}* in the absence of treatment, whereas in the treated group two situations were observed. First in mice that were not transgenic for *Rank* (*Rank^{Tg-}*), a graded increase in the number of TRAP positive cells at the alveolar bone surface was observed from the *Opg^{+/+}* to *Opg^{-/-}* mice, independently of eruption/root elongation status (Fig. 8). On the contrary, in the *Rank^{Tg+}* mice, regardless of the *Opg* genotype, a close to wild-type mice number of TRAP positive cells was observed at the alveolar bone surface (Fig. 8). Surprisingly, in contrast to the two situations observed for the number of TRAP positive cells at the alveolar bone surface, the number of TRAP positive cells at the root surface and in the root resorption lacunas of non-erupted teeth was similar for all genotypes, despite the fact that lacuna sizes were gradually greater with the loss of *Opg* alleles (Fig. 8). Other classical features of non-erupted teeth were observed for all genotypes, such as anatomical malformations and hypercementosis (Fig. 8).

In order to go further in the analyses of the craniofacial consequences of ZOL treatment in the different genotypes, the potentiality of a relationship between the severity of the dental phenotype and alteration to morphometric parameters was researched (Fig. 9). Skull length and the length of the facial region were analyzed dependent on the eruption status of the first upper molar (respectively Fig. 9B and C) and mandibular length dependent on the eruption status of the first lower molar (Fig. 9D). The table (Fig. 9A) summarizes mouse distribution in the different genotypes according to dental eruption status. A clear relationship was observed between full molar eruption and the absence of alteration to the craniofacial parameters, while in all cases of defective eruption a significant reduction in the craniofacial parameters was observed (Fig. 9). Interestingly, taking into account that full eruption after ZOL treatment was observed only for the *Opg^{-/-}Rank^{Tg-}* and *Opg^{-/-}Rank^{Tg+}* genotypes, the few mice from those genotypes with defective eruption (red asterisk) were analyzed apart and revealed, as for all the other genotypes, a reduction in the craniofacial parameters (Fig. 9).

3.3. Appendicular and craniofacial skeletons of transgenic mice, with genetically-induced variations in OPG and RANK expression levels, were still differentially affected a long time (10 months) after the end of the treatment with ZOL.

In order to analyze the long-term consequences of ZOL administered to newborn mice, twelve mice (two for each genotype) were followed from birth until ten months of age using micro-CT scans of the tibia (Fig. 10) and head (Fig. 11). Unfortunately, at three and six months of age respectively five and three mice were sacrificed for ethical reasons due to the deterioration of their health consecutive to the development of abnormal massive neoplastic-like structures in

the proximal region of either upper or lower incisors (Fig. 11). Consequently, at ten months only four animals were analyzed using the same parameters as for the analyses carried out at one and half months. Two of these mice corresponded to *Opg^{+/-}\Rank^{Tg-}*, one to *Opg^{+/-}\Rank^{Tg+}* and one to *Opg^{-/-}\Rank^{Tg+}*. In order to analyze the consequences of the ZOL treatment during growth on the bone morphometric and mineral parameters at ten months, six untreated mice with the same genotypes were used as references.

Regarding the appendicular skeleton, the BV/TV analyses revealed that while this percentage was null for all untreated mice, it remained very high in *Opg^{+/-}\Rank^{Tg+}* and *Opg^{-/-}\Rank^{Tg+}* mice (Fig. 10A). In contrast, in the *Opg^{+/-}\Rank^{Tg-}* mice, this percentage was low compared to the values reported at one and half months (Fig. 10A). The TMD analyses revealed greater values in treated mice, except for the *Opg^{+/-}\Rank^{Tg+}* mice (Fig. 10A), in contrast with the situation at one and half months. Concerning the bone morphometric parameters of the tibia, with the exception of bone thickness (total length, external diameter and internal diameter), lower values were observed for the four treated mice compared to the untreated mice (Fig. 10B and C).

For the craniofacial skeleton, the micro-CT scans of the heads revealed that the eruption defects in both incisors and first molars were still present (Fig. 11A) with, in addition, the presence in three of the four treated mice of tumor-like structures associated with non-erupted upper incisors (red arrows in Fig. 11A). Morphometric analyses (Fig. 11B, C and D) revealed that all the treated mice (red dots) still had smaller measurements in all planes of growth (sagittal, vertical, maxillary and transversal) compared to untreated mice with the same genotypes (black dots), except for cranial vault length and the middle cranial vault (measurements F and H).

4. Discussion

The role of the RANKL, RANK, OPG triad in bone modeling and remodeling has been extensively documented [22,32]. N-BPs are some of the most potent inhibitors of these bone processes currently used in clinical practice [1,6,33]. Curiously, the potential relationship between the relative expression levels of the members of this triad and the intensity of the effects and side-effects of N-BPs on the skeleton has not been questioned until now. The main objective of the present research was thus to tackle such a relationship during growth (bone modeling) for zoledronic acid, focusing on expression levels in the bone microenvironment of the two receptors, RANK and OPG. The central hypothesis was that combining two transgenic mouse models, corresponding to an increase in expression levels of RANK in the monocyte/macrophage lineage (*Rank^{Tg}*) and a global decrease in OPG expression levels (*Opg^{KO}*), made it possible to obtain a gradual series of osteolytic microenvironments for identifying the impact of RANKL signaling activity levels on the effects and side-effects of zoledronic acid on a growing skeleton. Such combinations of transgenic mice have never been realized before and the first step was therefore to analyze the skeletal phenotypes associated with the six different genotypes (*Opg^{+/+}\Rank^{Tg-}*, *Opg^{+/+}\Rank^{Tg+}*, *Opg^{+/-}\Rank^{Tg-}*, *Opg^{+/-}\Rank^{Tg+}*, *Opg^{-/-}\Rank^{Tg-}* and *Opg^{-/-}\Rank^{Tg+}*) at the end of growth (one and a half months after birth).

4.1. Skeletal phenotypes associated with graded osteolytic genotypes at the end of growth.

The bone morphometric and mineral parameter analyses performed for the different

genotypes made it possible to obtain significant, previously unreported, findings regarding skeletal growth. Regardless of the genotype, the morphometric parameters of the long bones and craniofacial bones were similar, meaning that the different *Opg* and *Rank* osteolytic genotypes (bone osteolytic micro-environments) did not affect the size of the bones at the end of growth. Interestingly, this did not mean that the timing of skeleton growth was the same, as early alveolar bone modeling associated with tooth eruption and root elongation has previously been described for *Rank^{Tg}* [34], but that the final sizes of the bones were genetically determined and independent of osteolytic status during growth, as previously suggested [16].

In contrast to bone morphometric parameters, certain bone mineral parameters (BV/TV, Tb.N, and TMD) revealed differences at the end of growth (mainly in the craniofacial bones), more specifically in the *Opg^{-/-}* genotypes. For instance, in long bones the TMD, and in alveolar and basal bones the BV/TV, had lower values for *Opg^{-/-}* independently of *Rank* expression. These observations demonstrated that despite the absence of consequence on bone morphometry, the different osteolytic genotypes had impacts on bone mineral structure at the end of growth, which might influence the mechanical properties of bones and induce their premature wear during adulthood, with a high risk of fracture as seen in the *Opg^{-/-}Rank^{Tg+}* mouse in Figure 9A.

The histological analysis in craniofacial tissues showed a graded increase in the number of TRAP positive cells, proportional to the allelic reduction in *Opg* and the increase in *Rank*, validating the hypothesis of the existence of a graded osteolytic series associated with the different genotypes. This histological analysis also revealed that despite the normal eruption status of teeth observed regardless of the genotype, dental root structure was affected, specifically in the *Opg^{-/-}* mice, independently of *Rank* over-expression, with the presence of

lacunas of resorption in the root cervical area. In addition, a reduction in root diameter was present in the *Rank^{Tg}* mice, as previously reported [16,34]. Altogether, these data validated the importance of RANKL signaling in dental root formation through its implication in the communications between dental, periodontal and bone cells needed for harmonious and functional growth of the complex formed by the tooth and alveolar bone [16,34–36]. Interestingly, RANKL signaling was previously reported as being important later, in adulthood, for the homeostasis of dental and periodontal tissues. Root resorptions, cementum mineralization reduction, dentine hypertrophy with decreased size of the pulp chamber and severe alveolar bone resorptions have been described in *Opg^{-/-}* adult mice [37–40], while root and alveolar bone resorptions were reported in *Rank^{Tg}* mice [41]. In patients, idiopathic external resorption was reported in cases of Familial Expansile Osteolysis [27,42], and tooth loss and mandible deformities in early onset familial Paget disease [42–45]. Finally, RANKL signaling appeared to be important in all stages of the life of the complex formed by the tooth and its associated alveolar bone, from embryonic morphogenesis [46] through growth (present work) to adult homeostasis.

To summarize, the gradual allelic reduction in *Opg*, associated or not with the overexpression of *Rank*, made it possible to generate a series of transgenic mice with graded levels of RANKL signaling activity in the bone microenvironment. Analysis of the skeletal phenotype of these different mice at the end of growth revealed no difference concerning the bone morphometric parameters, while the bone mineral parameters were reduced in the absence of *Opg* (*Opg^{-/-}*) regardless of *Rank^{Tg}* status. Concerning the complex formed by the tooth and its associated alveolar bone, the absence of *Opg* was allied to root resorptions, and the over-

expression of *Rank* to a reduction in root diameter with, surprisingly, apparent independence of these two effects.

4.2. The effects and side-effects of ZOL on the growing skeleton of mice with different osteolytic genotypes.

In order to identify the impact of RANKL signaling activity levels on the effects and side-effects of ZOL on a growing skeleton, a protocol that mimicked those used in onco-pediatric patients was applied to the mice with different genotypes, and the skeletal phenotypes at the end of growth were established and compared. This experiment first revealed that regardless of the genotype considered, ZOL impacted the growing skeletons (morphometric as well as mineral and dental parameters). However, variations were observed between the different genotypes, confirming the hypothesis that genetically-achieved over-activation of RANKL signaling could deal with the effects and side-effects of ZOL on a growing skeleton. Surprisingly, no linear relationship was observed between the graded osteolytic levels and the intensity of the effects and side-effects at the end of growth. Indeed, the two different ways of increasing RANKL signaling, namely *Opg* invalidation and *Rank* over-expression, seemed to differentially impact the effects and side-effects of ZOL. For bone morphometric parameters, the absence of *Opg* (*Opg*^{-/-}) was the only situation in which the effect of ZOL was prevented regardless of *Rank*^{Tg} status. For bone mineral parameters (BV/TV, Tb.N and Tb.Th), two situations were observed. First, in the absence of *Rank* overexpression (*Rank*^{Tg-}), the bone mineral parameter values gradually decreased with *Opg* allelic reduction, close to the zero observed in non-treated mice. Secondly, in the *Rank*-overexpressing mice (*Rank*^{Tg+}), regardless of the *Opg* expression level, the bone mineral parameters were very high

compared to non-treated mice. Altogether, these results demonstrated that the genetically-achieved reduction in *Opg* expression was the only situation that made it possible to limit or reverse the effects and side-effects of ZOL by the end of pediatric growth. Interestingly, a similar consequence of *Opg* invalidation was reported for another inhibitor of bone resorption also used in clinical practice, Strontium [47]. The most surprising results in the ZOL-treated mice were contrary to the expected impacts of *Rank* over-expression on bone mineral parameters and the absence of effect on bone morphometric parameters. One explanation may come from the number of TRAP positive cells observed at the bone surface at the end of growth, which increased with *Opg* allelic loss, while being highly limited when *Rank* was over-expressed. This explanation, based on a more significant bone resorption capacity during the month following treatment (until the end of growth), was supported by the relationship observed between full tooth eruption and the unaffected sagittal growth of the skull, two independent processes that are highly sensitive to osteoclast activity. However, the underlying molecular mechanisms still need to be elucidated.

At least two hypotheses could be proposed to explain the differences in the effects and side-effects of ZOL on a growing skeleton between *Opg* allelic reduction and *Rank* over-expression. The first was linked to the existence of a third receptor for RANKL, called LGR4 [48]. This receptor was expressed by osteoclasts and osteoblasts [48–57] with a reverse function regarding the differentiation of those cells. Osteoblastogenesis was effectively shown to be stimulated by LGR4 activation whereas osteoclastogenesis was inhibited [48–51,54,57]. Interestingly, LGR4 expression was stimulated during osteoclastogenesis [48], as a target of NFATC1, and thus in response to RANK stimulation by RANKL, suggesting the presence of an auto-regulatory loop for the RANKL effect on osteoclasts. Moreover, LGR4 activation was

shown to control mature osteoclast survival by inducing apoptosis [48]. In the *Opg*^{-/-} mouse, the relative expression patterns of RANK and LGR4 during osteoclastogenesis until the mature and functional osteoclast stage had no reason to be affected, while in the *Rank*^{Tg+} mouse this was undoubtedly the case. This may explain the difference in the response to ZOL observed between the two genetically-achieved models of RANKL signaling over-activation.

The second hypothesis corresponded to a depletion of the osteoclast precursors in the *Rank*^{Tg+} mouse following the treatment with ZOL. This transgenic mouse corresponded to an over-expression of *Rank* driven by the promoter of Myeloid Related Protein 8 (MRP8, also known as S100A8) which induced in the bone marrow a significant increase in the pre-monocyte-macrophage population (CD11b⁺ Gr1⁻) over-expressing *Rank* [29,58]. Physiologically, osteoclastogenesis was achieved from the pre-monocyte-macrophage population (osteoclast precursors) by two successive inductions. The first corresponded to the binding of M-CSF to its receptor C-FMS, expressed at the surface of the precursors, which induced RANK expression, and the second to the binding of RANKL to RANK, making possible the fusion of the precursors into multinucleate osteoclastic cells (for review [59]). In the *Rank*^{Tg+} mouse, the ectopic presence of RANK in the precursors made possible accelerated osteoclastogenesis in response to RANKL inducing the osteolytic phenotype as previously described [16,34]. According to the facts that N-BPs (such as ZOL) induce an accumulation of giant osteoclasts unable to resorb the bone matrix at the bone surface [60–65] and a decrease in the number of macrophage precursors in the bone marrow [66], a depletion of RANK over-expressing precursors may be the result of the treatment with ZOL in the *Rank*^{Tg+} mice.

Further studies will be needed to validate or invalidate each of these hypotheses regarding the origin of the difference in the response to ZOL observed between the two genetically-achieved models of RANKL signaling over-activation.

To summarize, most of the effects and side-effects of ZOL on growing mouse skeletons observed at the end of pediatric growth appeared to be contingent on osteolytic bone levels associated with genetically-achieved graded over-activation of RANKL signaling. This was the case for the increase in bone mineral parameters, blockage of tooth eruption and reduced appendicular and craniofacial bone growth. However, this dependence was not linear and two situations emerged. Graded *Opg* invalidation reduced the effects and side-effects of ZOL, while *Rank* over-expression enforced them. Interestingly, when *Opg* invalidation was combined with *Rank* over-expression, the effects and side-effects revealed different susceptibilities. The morphometric parameters and tooth eruption were driven by the influence of *Opg* invalidation, and the bone mineral parameters by that of *Rank* over-expression. The basis of this dichotomy remains to be elucidated.

4.3. Long-term stability of the effects and side-effects of ZOL on growing skeletons.

Analysis of the consequences on the skeleton of pediatric treatment with ZOL at a distance from the end of the treatment (ten months of age) showed that most of the initially described effects and side-effects of ZOL on long and craniofacial bones persisted into adulthood, although in some cases there were differences in intensity depending on the genotypes. The bone morphometric parameters were still lower in the treated mice with respect to the genotypes, and the eruption defects were definitive as previously concluded [4,9]. Surprisingly,

the TMD had increased at ten months compared to one and half months in the treated groups, regardless of the genotype, reaching values globally higher than in non-treated animals (for instance, in treated *Opg^{+/-}Rank^{Tg}* mice 5.0 at ten months *versus* 3.8±0.3 at one and half months, whereas in the untreated animals, the values were respectively 4.65 and 4.5±0.4). However, the most remarkable results concerned the bone mineral parameters at ten months, for which the dichotomy between *Opg* invalidation and *Rank* over-expression still seemed to be present. Despite the small number of mice that survived up to ten months due to the development of neoplastic-like structures in the apical part of the continuously-growing incisors in the treated mice, the BV/TV and Tb.N increases induced by treatment with ZOL were close to the reverse at ten months, in the absence of *Rank* over-expression, while they were maintained at high levels in the presence of *Rank* over-expression.

To summarize, the consequences of treatment with ZOL on skeletons during growth were highly stable, as could be seen after ten months. The differences in skeletal phenotype associated with the different genotypes observed at the end of growth were also still present and often enforced, with *Opg* invalidation fostering normalization, while *Rank* over-expression maintained or exacerbated the situation.

The question of the origin of the different individual sensibilities to treatment with ZOL during growth have been addressed here, taking into consideration the RANKL signaling activity level as a major actor. Mice deficient for *Opg* and over-expressing *Rank* were mated to generate mice with graded levels of RANKL signaling activity. The skeletal phenotypes of these mice were established at the end of growth and at ten months, following either treatment or no treatment from postnatal days 1 to 7 with high doses of ZOL. The results

obtained demonstrated that the RANKL signaling activity level had important repercussions on the effects and side-effects of ZOL on the skeleton, but that these repercussions were not proportional to the levels of activity but rather dependent on the way the RANKL signaling was boosted. *Opg* invalidation made it possible to reduce these effects and side-effects, while *Rank* over-expression enforced them. Finally, these repercussions appeared to be stable over time, although with a noticeable improvement in the mice with allelic reductions in *Opg* but not when *Rank* was over-expressed.

5. Abbreviations

EDTA: Ethylene-diamine-tetraacetic acid; Micro-CT: micro-computed tomography; OPG: osteoprotegerin; RANK: receptor activator of nuclear factor kappa B; RANKL: RANK ligand; TRAP: tartrate-resistant acid phosphatase; ZOL: zoledronic acid.

6. Acknowledgements

The authors would like to thank G. Hamery and J. Pajot from the Therapeutic Experimental Unit (Nantes, France) for their technical assistance. AG was supported by the CAPES Foundation, Ministry of Education of Brazil, Brasília, Brazil.

7. Contributions

Designing research studies: JWVF, BC, DH, FR and FL.

Conducting experiments: JWVF, AG and FL.

Acquiring data: JWVF and FL.

Analyzing data: JWVF, BC, AG, DH, FR and FL.

Providing reagents: CGM and DH.

Writing the manuscript: JWVF, BC and FL.

8. Competing interests

The authors have declared that there is no conflict of interest.

9. Funding

The project received the financial support of the French National Cancer Institute (Funding INCa-6001), the “Ligue Nationale Contre le Cancer” [Equipe LIGUE 2012 (DH) and Ligue régionale grand-ouest comités 22, 44 and 49 (FL)] and the Bone Cancer Research Trust, UK (research project number 144681).

10. References

- [1] J.W. Vargas-Franco, B. Castaneda, F. Rédiní, D.F. Gómez, D. Heymann, F. Lézot, Paradoxical side effects of bisphosphonates on the skeleton: What do we know and what can we do?, *Journal of Cellular Physiology*. 233 (2018) 5696–5715. doi:10.1002/jcp.26465.
- [2] I. Vuorimies, H. Arponen, H. Valta, O. Tiesalo, M. Ekholm, H. Ranta, M. Evälahti, O. Mäkitie, J. Waltimo-Sirén, Timing of dental development in osteogenesis imperfecta patients with and without bisphosphonate treatment, *Bone*. 94 (2017) 29–33. doi:10.1016/j.bone.2016.10.004.
- [3] M. Hernandez, B. Phulpin, L. Mansuy, D. Droz, Use of new targeted cancer therapies in children: effects on dental development and risk of jaw osteonecrosis: a review, *Journal of Oral Pathology & Medicine*. 46 (2017) 321–326. doi:10.1111/jop.12516.
- [4] F. Lézot, J. Chesneau, S. Battaglia, R. Brion, B. Castaneda, J.-C.J.-C. Farges, D. Heymann, F. Rédiní, Preclinical evidence of potential craniofacial adverse effect of zoledronic acid in pediatric patients with bone malignancies, *Bone*. 68 (2014) 146–152. doi:10.1016/j.bone.2014.08.018.
- [5] T. Hiraga, T. Ninomiya, A. Hosoya, H. Nakamura, Administration of the bisphosphonate zoledronic acid during tooth development inhibits tooth eruption and formation and induces dental abnormalities in rats, *Calcified Tissue International*. 86 (2010) 502–510. doi:10.1007/s00223-010-9366-z.
- [6] R.N. Bhatt, S.A. Hibbert, C.F. Munns, The use of bisphosphonates in children: Review of the literature and guidelines for dental management, *Australian Dental Journal*. 59 (2014) 9–19. doi:10.1111/adj.12140.
- [7] E.J. Smith, D.G. Little, J.N. Briody, A. McEvoy, N.C. Smith, J.A. Eisman, E.M. Gardiner, Transient disturbance in physeal morphology is associated with long-term effects of nitrogen-containing bisphosphonates in growing rabbits., *Journal of Bone and Mineral Research : The Official Journal of the American Society for Bone and Mineral Research*. 20 (2005) 1731–1741. doi:10.1359/JBMR.050604.
- [8] C.F. Munns, F. Rauch, R. Travers, F.H. Glorieux, Effects of Intravenous Pamidronate Treatment in Infants With Osteogenesis Imperfecta: Clinical and Histomorphometric Outcome, *Journal of Bone and Mineral Research*. 20 (2005) 1235–1243. doi:10.1359/JBMR.050213.

- [9] F. Lézot, J. Chesneau, B. Navet, B. Gobin, J. Amiaud, Y. Choi, H. Yagita, B. Castaneda, A. Berdal, C. Mueller, F. Rédini, D. Heymann, Skeletal consequences of RANKL-blocking antibody (IK22-5) injections during growth: mouse strain disparities and synergic effect with zoledronic acid., *Bone*. 73 (2015) 51–59. doi:10.1016/j.bone.2014.12.011.
- [10] M. Pazianas, B. Abrahamsen, Safety of bisphosphonates, *Bone*. 49 (2011) 103–110. doi:10.1016/j.bone.2011.01.003.
- [11] L. Sinigaglia, M. Varenna, S. Casari, Pharmacokinetic profile of bisphosphonates in the treatment of metabolic bone disorders, *Clinical Cases in Mineral and Bone Metabolism*. 4 (2007) 30–36.
- [12] M.R. Allen, D.B. Burr, Bisphosphonate effects on bone turnover, microdamage, and mechanical properties: What we think we know and what we know that we don't know, *Bone*. 49 (2011) 56–65. doi:10.1016/j.bone.2010.10.159.
- [13] K.M. Kim, Y. Rhee, Y. Kwon, T. Kwon, J.K. Lee, D. Kim, D. Kim, Medication Related Osteonecrosis of the Jaw: 2015 Position Statement of the Korean Society for Bone and Mineral Research and the Korean Association of Oral and Maxillofacial Surgeons, *J Bone Metab*. 22 (2015) 151–165. doi:10.11005/jbm.2015.22.4.151.
- [14] M.C. Walsh, Y. Choi, Biology of the RANKL-RANK-OPG System in Immunity, Bone, and Beyond., *Frontiers in Immunology*. 5 (2014) 1–11. doi:10.3389/fimmu.2014.00511.
- [15] L. Ginaldi, M. De Martinis, Osteoimmunology and Beyond, *Current Medicinal Chemistry*. 23 (2016) 1–21. doi:10.2174/0929867323666160907.
- [16] B. Castaneda, Y. Simon, D. Ferbus, B. Robert, J. Chesneau, C. Mueller, A. Berdal, F. Lézot, Role of RANKL (TNFSF11)-dependent osteopetrosis in the dental phenotype of *Msx2* null mutant mice, *PLoS ONE*. 8 (2013) 1–9. doi:10.1371/journal.pone.0080054.
- [17] B. Navet, J.W. Vargas-franco, A. Gama, J. Amiaud, Y. Choi, H. Yagita, C.G. Mueller, F. Rédini, D. Heymann, B. Castaneda, F. Lézot, Maternal RANKL Reduces the Osteopetrotic Phenotype of Null Mutant Mouse Pups, *Journal of Clinical Medicine*. 7 (2018) 1–13. doi:10.3390/jcm7110426.
- [18] Khosla S, Minireview: the opg/rankl/rank system., *Endocrinology*. 142 (2001) 5050–5055. doi:10.1210/endo.142.12.8536.
- [19] V. Nagy, J.M. Penninger, The RANKL-RANK Story, *Gerontology*. 61 (2015) 534–542. doi:10.1159/000371845.

- [20] S. Theoleyre, Y. Wittrant, S.K. Tat, Y. Fortun, F. Redini, D. Heymann, The molecular triad OPG/RANK/RANKL: Involvement in the orchestration of pathophysiological bone remodeling, *Cytokine and Growth Factor Reviews*. 15 (2004) 457–475. doi:10.1016/j.cytogfr.2004.06.004.
- [21] W. Liu, X. Zhang, Receptor activator of nuclear factor- κ B ligand (RANKL)/RANK/osteoprotegerin system in bone and other tissues (Review), *Molecular Medicine Reports*. 11 (2015) 3212–3218. doi:10.3892/mmr.2015.3152.
- [22] B.F. Boyce, L. Xing, Functions of RANKL/RANK/OPG in bone modeling and remodeling, *Archives of Biochemistry and Biophysics*. 473 (2008) 139–146. doi:10.1016/j.abb.2008.03.018.
- [23] L. Bagan, Y. Jiménez, M. Leopoldo, A. Rubert, J. Bagan, Serum levels of RANKL and OPG, and the RANKL/OPG ratio in bisphosphonate-related osteonecrosis of the jaw: Are they useful biomarkers for the advanced stages of osteonecrosis?, *Medicina Oral, Patología Oral y Cirugía Bucal*. 22 (2017) 542–547. doi:10.4317/medoral.22128.
- [24] C. Di Nisio, V.L. Zizzari, S. Zara, M. Falconi, G. Teti, G. Tetè, a. Nori, V. Zavaglia, a. Cataldi, RANK/RANKL/OPG signaling pathways in necrotic jaw bone from bisphosphonate-treated subjects, *European Journal of Histochemistry*. 59 (2015) 45–50. doi:10.4081/ejh.2015.2455.
- [25] A.E. Hughes, S.H. Ralston, J. Marken, C. Bell, H. MacPherson, R.G.H. Wallace, W. van Hul, M.P. Whyte, K. Nakatsuka, L. Hovy, D.M. Anderson, Mutations in TNFRSF11A, affecting the signal peptide of RANK, cause familial expansile osteolysis, *Nature Genetics*. 24 (2000) 45–48. doi:10.1038/71667.
- [26] M.P. Whyte, S.E. Brecht, P.M. Flinnegan, L. Jones, M.N. Podgornik, W.H. McAlister, S. Mumm, Osteoprotegerin Deficiency and Juvenile Paget's Disease, *N Engl J Med*. 347 (2002) 175–184.
- [27] M.P. Whyte, Mendelian Disorders of RANKL/OPG/RANK/NF- κ B Signaling, in: R. V. Thakker, M.P. Whyte, J.T. Eisman, I. Akashi (Eds.), *Genetics of Bone Biology and Skeletal Disease*, Second Edi, Elsevier Inc., London, 2016: pp. 453–468. doi:10.1016/B978-0-12-804182-6/00026-5.
- [28] M.T. Drake, B.L. Clarke, S. Khosla, Bisphosphonates: Mechanism of Action and Role in Clinical Practice REVIEW, *Mayo Clinic Proceedings*. 83 (2008) 1032–1045.

doi:10.4065/83.9.1032.

- [29] V. Duheron, E. Hess, M. Duval, M. Decossas, B. Castaneda, J.E. Klöpper, Receptor activator of NF- κ B (RANK) stimulates the proliferation of epithelial cells of the epidermo-pilosebaceous unit, *Proceedings of the National Academy of Sciences of the United States of America*. 108 (2011) 5342–5347. doi:10.1073/pnas.1013054108/-/DCSupplemental.www.pnas.org/cgi/doi/10.1073/pnas.1013054108.
- [30] S.R. Vora, E.D. Camci, T.C. Cox, Postnatal ontogeny of the cranial base and craniofacial skeleton in male C57BL/6J mice: A reference standard for quantitative analysis, *Frontiers in Physiology*. 6 (2016) 1–3. doi:10.3389/fphys.2015.00417.
- [31] Y. Simon, A. Marchadier, M.K. Riviere, K. Vandamme, F. Koenig, F. Lezot, A. Trouve, C.L. Benhamou, J.L. Saffar, A. Berdal, J.R. Nefussi, Cephalometric assessment of craniofacial dysmorphologies in relation with Msx2 mutations in mouse, *Orthodontics and Craniofacial Research*. 17 (2014) 92–105. doi:10.1111/ocr.12035.
- [32] M.R. Allen, D.B. Burr, Bone modeling and remodeling, in: D.B. Burr, M.R. Allen (Eds.), *Basic and Applied Bone Biology*, Elsevier Inc., 2013: pp. 75–90. doi:10.1016/B978-0-12-416015-6.00004-6.
- [33] J.Y. Reginster, A. Neuprez, N. Dardenne, C. Beudart, P. Emonts, O. Bruyere, Efficacy and safety of currently marketed anti-osteoporosis medications., *Best Practice & Research. Clinical Endocrinology & Metabolism*. 28 (2014) 809–34. doi:10.1016/j.beem.2014.09.003.
- [34] B. Castaneda, Y. Simon, J. Jacques, E. Hess, Y.-W.W. Choi, C. Blin-Wakkach, C. Mueller, A. Berdal, F. Lézot, Bone resorption control of tooth eruption and root morphogenesis: Involvement of the receptor activator of NF- κ B (RANK), *Journal of Cellular Physiology*. 226 (2011) 74–85. doi:10.1002/jcp.22305.
- [35] A. Gama, B. Navet, J.W. Vargas, B. Castaneda, F. Lézot, Bone resorption: An actor of dental and periodontal development?, *Frontiers in Physiology*. 6 (2015) 1–7. doi:10.3389/fphys.2015.00319.
- [36] A. Berdal, B. Castaneda, M. Aïoub, J.R. Néfussi, C. Mueller, V. Descroix, F. Lézot, Osteoclasts in the dental microenvironment: A delicate balance controls dental histogenesis, *Cells Tissues Organs*. 194 (2011) 238–243. doi:10.1159/000324787.
- [37] Z.F. Sheng, W. Ye, J. Wang, C.H. Li, J.H. Liu, Q.C. Liang, S. Li, K. Xu, E.Y. Liao, OPG

knockout mouse teeth display reduced alveolar bone mass and hypermineralization in enamel and dentin, *Archives of Oral Biology*. 55 (2010) 288–293. doi:10.1016/j.archoralbio.2010.02.007.

[38] M. Koide, Y. Kobayashi, T. Ninomiya, M. Nakamura, H. Yasuda, Y. Arai, N. Okahashi, N. Yoshinari, N. Takahashi, N. Udagawa, Osteoprotegerin-deficient male mice as a model for severe alveolar bone loss: comparison with RANKL-overexpressing transgenic male mice., *Endocrinology*. 154 (2013) 773–82. doi:10.1210/en.2012-1928.

[39] Y. Liu, H. Du, Y. Wang, M. Liu, S. Deng, L. Fan, L. Zhang, Y. Sun, Q. Zhang, Osteoprotegerin-Knockout Mice Developed Early Onset Root Resorption, *Journal of Endodontics*. 42 (2016) 1516–1522. doi:10.1016/j.joen.2016.07.008.

[40] Y. Wang, M. Liu, S. Deng, X. Sui, L. Fan, Q. Zhang, Osteoprotegerin deficiency causes morphological and quantitative damage in epithelial rests of Malassez, *Journal of Molecular Histology*. 49 (2018) 329–338. doi:10.1007/s10735-018-9771-6.

[41] B. Sojod, D. Chateau, C.G. Mueller, S. Babajko, A. Berdal, F. Lézot, B. Castañeda, RANK / RANKL / OPG Signalization Implication in Periodontitis : New Evidence from a RANK Transgenic Mouse Model, *Front. Physiol*. 8 (2017) 1–12. doi:10.3389/fphys.2017.00338.

[42] A.L. Schafer, S. Mumm, I. El-Sayed, W.H. McAlister, A.E. Horvai, A.M. Tom, E.C. Hsiao, F. V. Schaefer, M.T. Collins, M.S. Anderson, M.P. Whyte, D.M. Shoback, Panostotic expansile bone disease with massive jaw tumor formation and a novel mutation in the signal peptide of RANK, *Journal of Bone and Mineral Research*. 29 (2014) 911–921. doi:10.1002/jbmr.2094.

[43] K. Nakatsuka, Y. Nishizawa, S.H. Ralston, Phenotypic Characterization of Early Onset Paget's Disease of Bone Caused by a 27-bp Duplication in the TNFRSF11A Gene, *Journal of Bone and Mineral Research*. 18 (2003) 1381–1385. doi:https://aplicacionesbiblioteca.udea.edu.co:4231/10.1359/jbmr.2003.18.8.1381.

[44] P.L. Riches, Y. Imanishi, K. Nakatsuka, S.H. Ralston, Clinical and Biochemical Response of TNFRSF11A-Mediated Early-Onset Familial Paget Disease to Bisphosphonate Therapy, *Calcified Tissue International*. 83 (2008) 272–275. doi:10.1007/s00223-008-9177-7.

[45] Y.-H. Ke, H. Yue, J.-W. He, Y.-J. Liu, Z.-L. Zhang, Early onset Paget's disease of bone caused by a novel mutation (78dup27) of the TNFRSF11A gene in a Chinese family, *Acta Pharmacologica Sinica*. 30 (2009) 1204–1210. doi:10.1038/aps.2009.90.

- [46] A. Ohazama, J.-M. Courtney, P.T. Sharpe, *Opg*, *Rank*, and *Rankl* in Tooth Development: Co-ordination of Odontogenesis and Osteogenesis, *Journal of Dental Research*. 83 (2004) 241–244. doi:10.1177/154405910408300311.
- [47] S. Peng, X.S. Liu, G. Zhou, Z. Li, K.D.K. Luk, X.E. Guo, W.W. Lu, Osteoprotegerin deficiency attenuates strontium-mediated inhibition of osteoclastogenesis and bone resorption, *Journal of Bone and Mineral Research*. 26 (2011) 1272–1282. doi:10.1002/jbmr.325.
- [48] J. Luo, Z. Yang, Y. Ma, Z. Yue, H. Lin, G. Qu, J. Huang, W. Dai, C. Li, C. Zheng, L. Xu, H. Chen, J. Wang, D. Li, S. Siwko, J.M. Penninger, G. Ning, J. Xiao, M. Liu, LGR4 is a receptor for RANKL and negatively regulates osteoclast differentiation and bone resorption, *Nature Medicine*. 22 (2016) 539–549. doi:10.1038/nm.4076.
- [49] J. Wang, B. Fu, F. Lu, X. Hu, J. Tang, L. Huang, Inhibitory activity of linarin on osteoclastogenesis through receptor activator of nuclear factor κ B ligand-induced NF- κ B pathway, *Biochemical and Biophysical Research Communications*. 495 (2018) 2133–2138. doi:10.1016/j.bbrc.2017.12.091.
- [50] X. Liu, X. Xu, MicroRNA-137 dysregulation predisposes to osteoporotic fracture by impeding ALP activity and expression via suppression of leucine-rich repeat-containing G-protein-coupled receptor 4 expression, *International Journal of Molecular Medicine*. 42 (2018) 1026–1033. doi:10.3892/ijmm.2018.3690.
- [51] R. Matsuike, H. Tanaka, K. Nakai, M. Kanda, M. Nagasaki, F. Murakami, C. Shibata, K. Mayahara, A. Nakajima, N. Tanabe, T. Kawato, M. Maeno, N. Shimizu, Continuous application of compressive force induces fusion of osteoclast-like RAW264.7 cells via upregulation of RANK and downregulation of LGR4, *Life Sciences*. 201 (2018) 30–36. doi:10.1016/j.lfs.2018.03.038.
- [52] G.X. Shi, X.F. Zheng, C. Zhu, B. Li, Y.R. Wang, S.D. Jiang, L.S. Jiang, Evidence of the role of R-spondin 1 and its receptor Lgr4 in the transmission of mechanical stimuli to biological signals for bone formation, *International Journal of Molecular Sciences*. 18 (2017) 5–7. doi:10.3390/ijms18030564.
- [53] G.-X. Shi, W.-W. Mao, X.-F. Zheng, L.-S. Jiang, The role of R-spondins and their receptors in bone metabolism, *Progress in Biophysics and Molecular Biology*. 122 (2016) 93–100. doi:10.1016/j.pbiomolbio.2016.05.012.
- [54] F. Cong, N. Wu, X. Tian, J. Fan, J. Liu, T. Song, H. Fu, MicroRNA-34c promotes

osteoclast differentiation through targeting LGR4, *Gene*. 610 (2017) 1–8. doi:10.1016/j.gene.2017.01.028.

[55] C. Pawaputanon Na Mahasarakham, Y. Izu, K. Nishimori, Y. Izumi, M. Noda, Y. Ezura, Lgr4 Expression in Osteoblastic Cells Is Suppressed by Hydrogen Peroxide Treatment, *Journal of Cellular Physiology*. 232 (2017) 1761–1766. doi:10.1002/jcp.25684.

[56] C. Pawaputanon Na Mahasarakham, Y. Ezura, M. Kawasaki, A. Smriti, S. Moriya, T. Yamada, Y. Izu, A. Nifuji, K. Nishimori, Y. Izumi, M. Noda, BMP-2 Enhances Lgr4 Gene Expression in Osteoblastic Cells, *Journal of Cellular Physiology*. 231 (2016) 887–895. doi:10.1002/jcp.25180.

[57] C. Zhu, X.-F. Zheng, Y.-H. Yang, B. Li, Y.-R. Wang, S.-D. Jiang, L.-S. Jiang, LGR4 acts as a key receptor for R-spondin 2 to promote osteogenesis through Wnt signaling pathway, *Cellular Signalling*. 28 (2016) 989–1000. doi:10.1016/j.cellsig.2016.04.010.

[58] E. Hess, V. Duheron, M. Decossas, F. Lezot, A. Berdal, S. Chea, R. Golub, M.R. Bosisio, S.L. Bridal, Y. Choi, H. Yagita, C.G. Mueller, RANKL Induces Organized Lymph Node Growth by Stromal Cell Proliferation, *The Journal of Immunology*. 188 (2012) 1245–1254. doi:10.4049/jimmunol.1101513.

[59] T. Ono, T. Nakashima, Recent advances in osteoclast biology, *Histochemistry and Cell Biology*. 149 (2018) 325–341. doi:10.1007/s00418-018-1636-2.

[60] F.C. Ko, L. Karim, D.J. Brooks, M.L. Bouxsein, M.B. Demay, Bisphosphonate Withdrawal: Effects on Bone Formation and Bone Resorption in Maturing Male Mice, *Journal of Bone and Mineral Research*. 32 (2017) 814–820. doi:10.1002/jbmr.3052.

[61] F. Mac-Way, A. Trombetti, C. Noel, M.H. Lafage-Proust, Giant osteoclasts in patients under bisphosphonates, *BMC Clinical Pathology*. 14 (2014) 1–5. doi:10.1186/1472-6890-14-31.

[62] S. Kuroshima, V.A.A. Go, J. Yamashita, Increased numbers of nonattached osteoclasts after long-term zoledronic acid therapy in mice, *Endocrinology*. 153 (2012) 17–28. doi:10.1210/en.2011-1439.

[63] R.S. Weinstein, P.K. Roberson, S.C. Manolagas, Giant Osteoclast Formation and Long-Term Oral Bisphosphonate Therapy, *The New England Journal of Medicine*. 360 (2009) 53–62. doi:https://aplicacionesbiblioteca.udea.edu.co:4231/10.1056/NEJMoa0802633.

[64] N. Jain, R.S. Weinstein, Giant osteoclasts after long-term bisphosphonate therapy:

diagnostic challenges, *Nature Reviews Rheumatology*. 5 (2009) 341–346. doi:10.1038/nrrheum.2009.87.

[65] L.A. Córdova, F. Guilbaud, J. Amiaud, S. Battaglia, C. Charrier, F. Lezot, B. Piot, F. Redini, D. Heymann, Severe compromise of preosteoblasts in a surgical mouse model of bisphosphonate-associated osteonecrosis of the jaw, *Journal of Cranio-Maxillofacial Surgery*. 44 (2016) 1387–1394. doi:10.1016/j.jcms.2016.07.015.

[66] N.D. Escudero, P.M. Mandalunis, Influence of Bisphosphonate Treatment on Medullary Macrophages and Osteoclasts: An Experimental Study, *Bone Marrow Research*. 2012 (2012) 1–8. doi:10.1155/2012/526236.

11. Figure Legends

Figure 1: Zoledronic acid (ZOL) administration protocol. From day one after birth mouse pups received four subcutaneous injections of ZOL at the dose of 50 μ g/kg at intervals of two days. Genotypes were determined at 1 month on tail biopsies by PCR on extracted genomic DNA. At one and half months, some of the treated mice were sacrificed to analyze the skeletal phenotypes at the end of growth. Twelve mice were maintained until ten months, with control micro-tomography every two months, to analyze the skeletal phenotypes at a distance from the treatment.

Figure 2: Analyses of bone morphometric and mineral parameters.

To analyze the effects of ZOL on long bone morphometric parameters (A), the tibia was measured in its length, width and thickness using specific reference dots making it possible to determine different values, named A to D. To analyze the effects of ZOL on craniofacial morphometric parameters (A), the skull was measured in all its planes using landmarks that made it possible to determine 8 representative measurements, named E to L. A phantom of known size (5mm) was used to calibrate and standardize all the measurements in CTVox and IMAGE-J software.

To analyze the effects of ZOL on long bone mineral parameters (B), a region of interest was chosen in the region of the tibia diaphysis, localized precisely 200 μ m over the furcation between tibia and fibula. The TMD (tissue mineral density) was measured for cortical bone (purple color), and the BV/TV (bone volume/tissue volume), Tb.N (trabecular number) and

Tb.Th (trabecular thickness) were measured for trabecular-like bone (green color). To analyze the effect of ZOL on craniofacial bone mineral parameters (B), eight regions of interest were chosen, four in the upper and four in the lower maxillary, corresponding to the inter-radicular areas of the first molars for alveolar bone (red color) and the underlying dental crypt areas for basal bone (blue color). The BV/TV (bone volume/tissue volume), Tb.N (trabecular number) and Tb.Th (trabecular thickness) were measured for both alveolar and basal bones.

Figure 3: Comparative analysis of long bone morphometric parameters between mice with different genotypes, treated or not with ZOL.

Tibia length (A), tibia external width (B), tibia internal width (C), and tibia cortical thickness (D) presented no significant difference between non-treated mice regardless of the genotype. In treated mice, tibia length (A), tibia external width (B), and tibia internal width (C) were significantly reduced for *Opg^{+/+}\Rank^{Tg-}*, *Opg^{+/-}\Rank^{Tg-}* and *Opg^{+/-}\Rank^{Tg+}* mice compared to untreated animals with respect to the genotype. The cortical thickness (D) was unaffected by the treatment with ZOL, regardless of the genotype considered. None of the parameters were affected by the treatment with ZOL in *Opg^{-/-}\Rank^{Tg-}* and *Opg^{-/-}\Rank^{Tg+}* mice (A-D). ns: not significant; *: P<0.05; **: P<0.01; ***: P<0.001; ****: P<0.0001.

Figure 4: Comparative analysis of long bone mineral parameters between mice with different genotypes, treated or not with ZOL.

Micro-CT scan sections in the sagittal and axial planes of the tibias with different genotypes with and without treatment were presented. Axial sections were realized in the diaphysis region of the tibias (the most affected by the ZOL treatment protocol chosen) in which

measurements of mineral parameters were made. The color density range revealed visually identifiable changes in the different structures. In the absence of treatment, the bone mineral parameters (BV/TV, Tb.N and Tb.Th) were null and the TMD around 4.4 gr/cm³ except in *Opg*^{-/-} (regardless of *Rank*^{Tg} status), for which the TMD was around 3.6 gr/cm³. In the treated group, the TMD was not significantly affected compared to the untreated group in respect to each genotype, while two situations emerged for the bone mineral parameters. In the absence of RANK over-expression (*Rank*^{Tg}), the BV/TV and Tb.N values decreased following the *Opg* allelic decrease, while in the presence of RANK over-expression (*Rank*^{Tg+}), these parameters were high.

Figure 5: Comparative analysis of craniofacial morphometric parameters between mice with different genotypes, treated or not with ZOL.

Measurements were carried out in the sagittal (A, B, C, F, G), vertical (D, E) and transversal (H) planes. In the absence of treatment, no difference was observed regardless of the measurement considered between the different genotypes, with the exception of facial height, which was significantly increased in the *Opg*^{-/-}/*Rank*^{Tg} mice (E). In the treated group, none of the parameters measured were significantly affected in the *Opg*^{-/-} mice regardless of *Rank*^{Tg} status, while for all the other genotypes the sagittal parameters were significantly reduced and the vertical and transversal ones unaffected. ns: not significant; *: P<0.05; **: P<0.01; ***: P<0.001; ****: P<0.0001.

Figure 6: Comparative analysis of craniofacial bone mineral parameters between mice with different genotypes, treated or not with ZOL.

Alveolar (A, C, E) and basal (B, D, F) maxillary bone mineral parameters were measured. In the absence of treatment, a graded decrease in the BV/TV and Tb.Th was observed in the alveolar bone (A, E) following the genotype severity in terms of osteolytic potential, while the Tb.N was stable except in *Opg*^{-/-}*Rank*^{Tg-} mice (C). In the basal bone, all parameters were significantly lower in the *Opg*^{-/-}*Rank*^{Tg-} mice and only the BV/TV in the *Opg*^{-/-}*Rank*^{Tg+} mice, while no difference was observed for the other genotypes (B, D, F). After treatment, the BV/TV and Tb.N were significantly increased in the basal bone regardless of the genotype considered (B, D), while the Tb.Th was significantly increased only in the basal bone of mice that did not over-express RANK (*Rank*^{Tg-}). ns: not significant; *: P<0.05; **: P<0.01; ***: P<0.001; ****: P<0.0001.

Figure 7: Comparative analysis of dental eruption between mice with different genotypes, treated or not with ZOL.

Lateral right and left side views and a frontal view of the micro-CT scans of heads (A) made it possible to classify the eruption of the first molars and incisors at three different stages: fully-erupted (yellow arrow-heads), partially-erupted (clear blue arrow-heads) and included (dark blue arrow-heads). In the absence of treatment, all teeth were fully-erupted regardless of the genotype considered (A), while after treatment the percentage of teeth in the different categories of the classification varied depending on the genotypes (B). A graded increase in the percentage of fully-erupted teeth was observed in relation to the severity of the genotype, with the *Opg*^{-/-}*Rank*^{Tg+} mice evidencing more fully-erupted teeth (B).

Figure 8: Comparative analysis of dento-alveolar histology between mice with different genotypes, treated or not with ZOL.

Masson trichrome staining and TRAP histo-enzymology were used on frontal sections of the head in the plane of the first mandibular molars for the different genotypes, treated or not with ZOL. In the absence of treatment, the first molars were fully-erupted and a graded increase in the number of TRAP positive cells at the alveolar bone surface was visible, depending on the severity of the genotype (black arrow-heads). Small root resorption lacunas were visible (yellow arrow-heads) in the *Opg*^{-/-} mice whether or not they over-expressed RANK. In the treated groups, the first molars were included, except in the *Opg*^{-/-} mice whether or not they over-expressed RANK. Root resorption lacunas were visible in all the included molars (yellow arrow-heads) while surprisingly not in all the fully-erupted molars, despite the fact that those teeth belonged to *Opg*^{-/-} mice. Enlargements of the views of the apical regions made it possible to observe a graded increase in the TRAP staining at the alveolar bone surface (black arrow-heads) following the *Opg* allelic reduction, only in the absence of RANK over-expression (*Rank*^{Tg}). In the RANK-over-expressing (*Rank*^{Tg+}) mice, few TRAP positive cells were present at the alveolar bone surface regardless of eruption status.

Figure 9: Correlation between defective eruption and a reduction in craniofacial sagittal morphometric parameters. In order to establish the existence of a correlation between effective tooth eruption and normal craniofacial sagittal parameter measurements, skull length (B), facial region length (C) and mandibular length (D) measurements were reanalyzed based on the eruption status of the first molars independently of genotype (A). To deal with the fact that all fully-erupted molars (yellow) were observed only in *Opg*^{-/-} mice, the four cases of non-

fully-erupted molars in *Opg*^{-/-} mice (red stars) were analyzed separately. The results revealed a strict correlation between defective eruption and reductions in craniofacial morphometric sagittal parameters. Moreover, these parameters associated with the fully-erupted teeth of treated mice were not significantly different from those of untreated mice. ns: not significant; *: P<0.05; **: P<0.01; ***: P<0.001; ****: P<0.0001.








Figure 10: Remnant consequences of treatment with ZOL on bone morphometric and mineral parameters in tibias at ten months of age. Sagittal and axial micro-CT images of ten-month-old mouse tibias, corresponding to the three genotypes for which mice (N=4) survived tumor-like structures induced by ZOL treatment, were analyzed for bone mineral parameters compared to untreated mice (N=6) with the same genotypes (A). The TMD appeared slightly higher in the treated mice, except in *Opg*^{+/-}*Rank*^{Tg+}. Interestingly, the most significant difference was observed in the *Opg*^{-/-}*Rank*^{Tg+} mice. The BV/TV and Tb.N were back to low values for the *Opg*^{+/-}*Rank*^{Tg-}, close to the zero observed for untreated mice. In contrast, in RANK over-expressing mice, *Opg*^{+/-}*Rank*^{Tg+} and *Opg*^{-/-}*Rank*^{Tg+}, these parameters remained high. The Tb.Th was not null, but low in the treated mice. The bone morphometric parameters in the same mice were measured (B, C). Regardless of the genotype considered, tibia length (B), and the external and internal diameters (C) appeared to decrease in the treated mice. In contrast, bone thickness was not affected (C).

Figure 11: Remnant consequences of treatment with ZOL on dental eruption and craniofacial morphometric parameters at ten months of age. Lateral right and left side views and a frontal view of micro-CT scans of ten-month-old mouse heads (A) made it

possible to reveal that parts of the molars and incisors had still not erupted (blue arrow-heads) with repercussions on the morphology of the erupted teeth (yellow arrow-heads). Tumor-like structures associated with included, continuously growing incisors were also visible (red arrow-heads). The craniofacial morphometric parameters of the four mice treated with ZOL that survived up to ten months were measured and compared to those obtained for non-treated mice with the same genotypes (B, C, D). For the measurements of sagittal growth (B), total growth and facial length were clearly lower in treated mice while the differences were less obvious for cranial vault length. For the measurements of vertical growth (C), facial height seemed to be the only parameter reduced, except in the *Opg^{+/-}Rank^{Tg+}* mouse. For transversal growth (D), all parameters appeared to have decreased, although less significantly in the *Opg^{+/-}Rank^{Tg+}* mouse.

**PROTOCOL OF DRUG INJECTION
(DAY AFTER BIRTH)**

**PROTOCOL OF ANALYSES
(MONTHS AFTER BIRTH)**

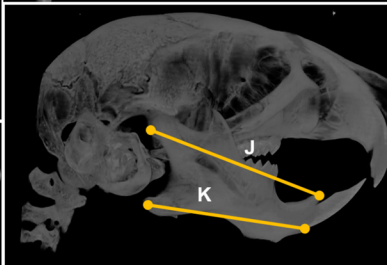
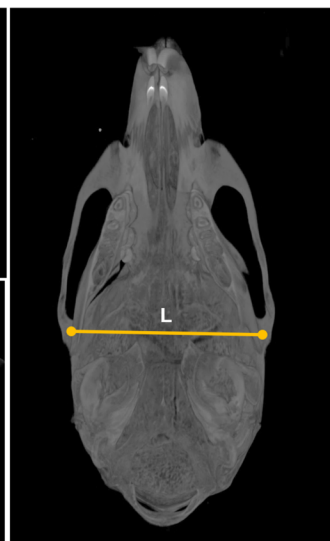
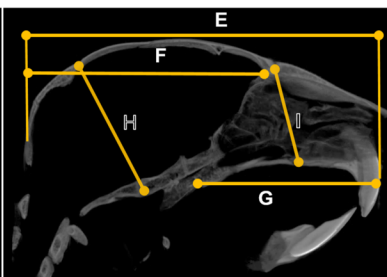
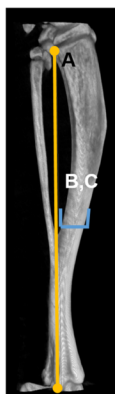
1 st	3 rd	5 th	7 th	1,5		10
					<p>Ten mice were followed each month</p>	
<p>4 Doses - 50ug/kg of ZOL, Injected subcutaneous</p>				<p>Euthanasia*</p>	<p>μ-CT</p>	<p>Euthanasia**</p>

* To analyze the side effects of ZOL at the end of growth.

**To analyze the side effects in adulthood.

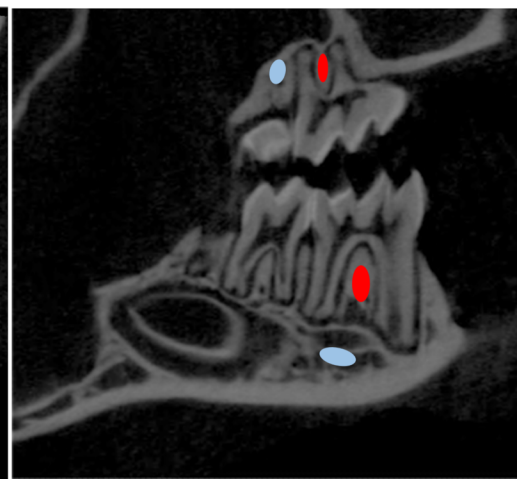
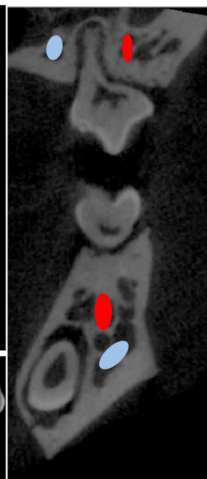
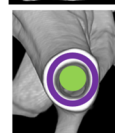
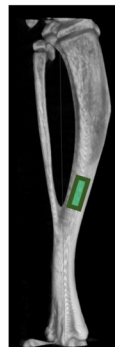
A: BONE MORPHOMETRIC PARAMETERS

SIZE	MARKS
1. Length growth	A: Medial condyle to medial Malleolus
2. Width growth	B: External Width C: Internal Width D: Thickness
3. Sagittal Growth (Antero – Posterior)	E: Total skull length F: Cranial vault length G: Facial region length
4. Vertical Growth	H: Middle cranial vault I: Facial height
5. Mandibular Growth	J: Mandibular length (superior) K: Mandibular length (inferior)
6. Width of the cranial vault	L: Inter-zygomatic root width

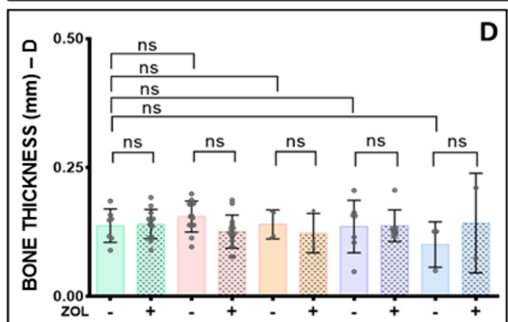
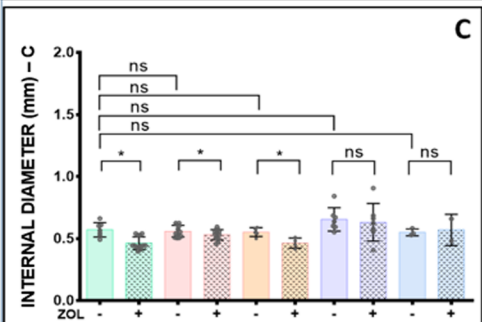
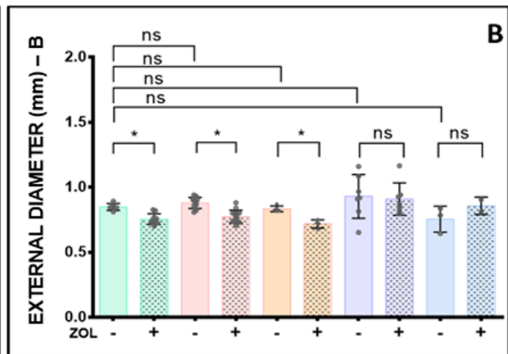
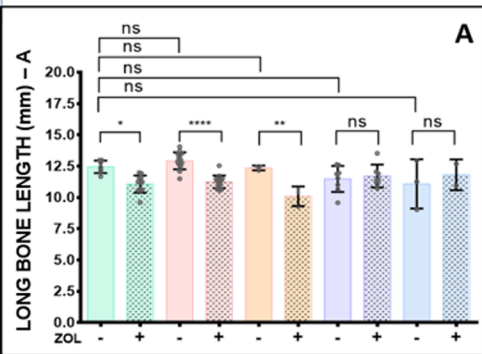


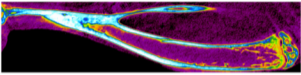
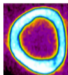
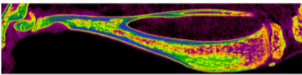
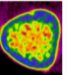
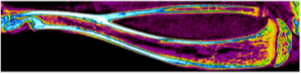
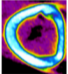
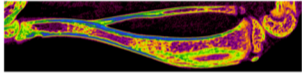
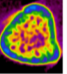
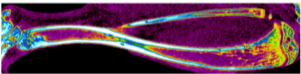
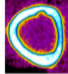
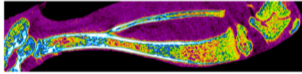
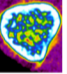
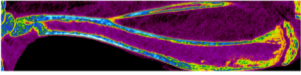
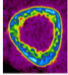
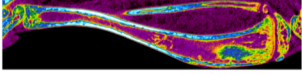
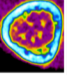
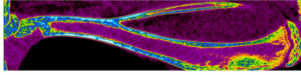
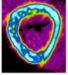
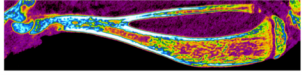
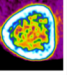
B: BONE MINERAL PARAMETERS

COLOR	MARKS
Red	Alveolar upper and lower maxillary bone
Blue	Basal upper and lower maxillary bone
Green	Trabecular long bone (Tibia)
Purple	Cortical long bone (Tibia)



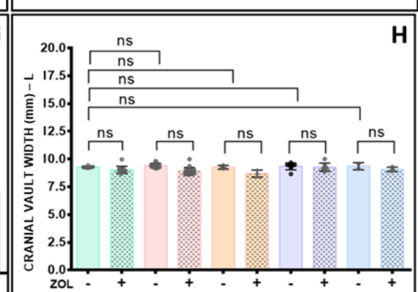
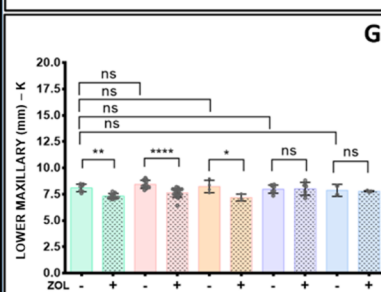
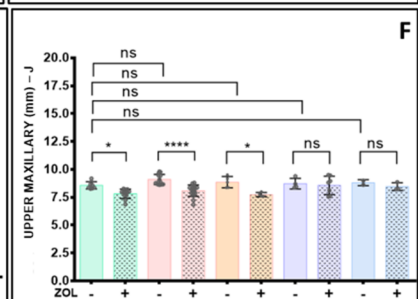
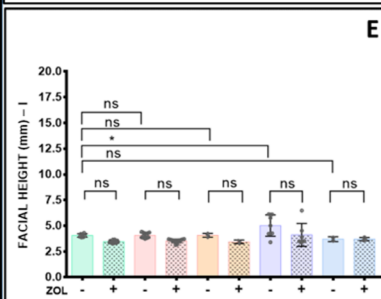
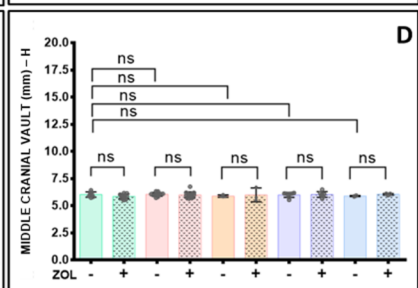
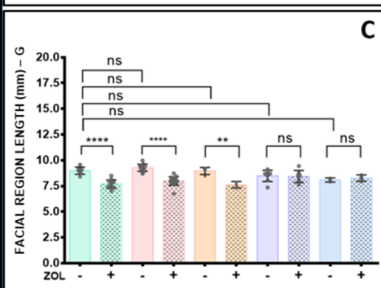
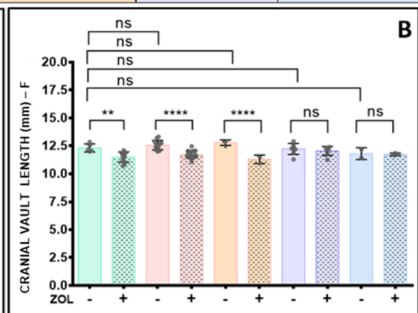
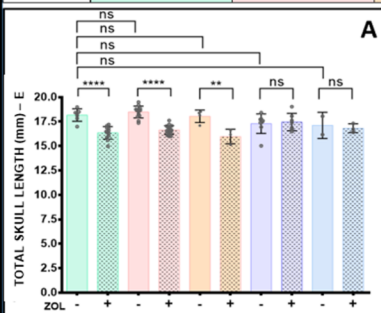
<i>Opg</i>	+/+	+/-	+/-	-/-	-/-
<i>Rank</i> ^{Tg}	-	-	+	-	+



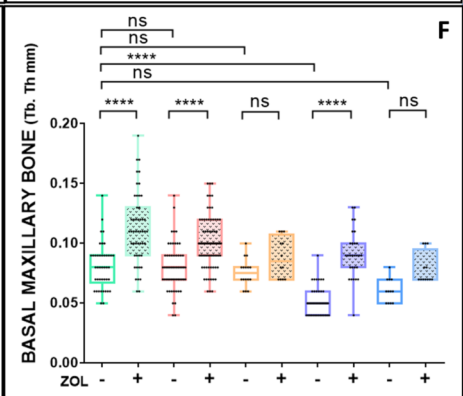
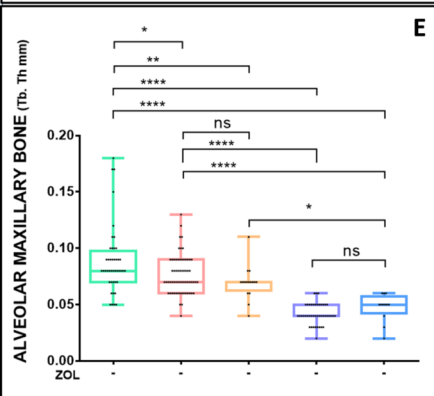
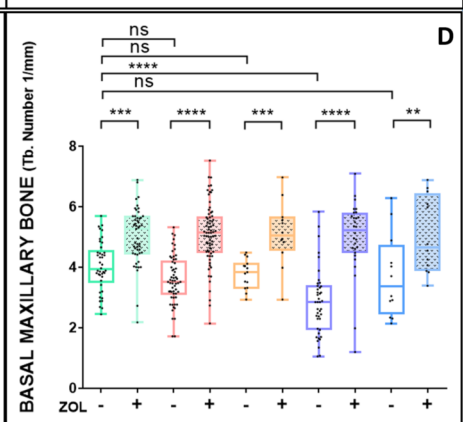
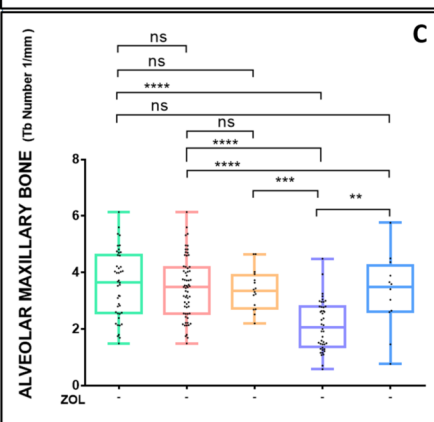
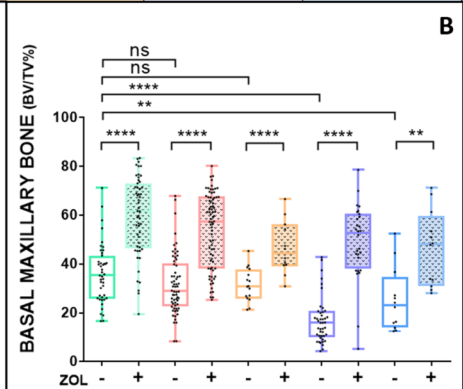
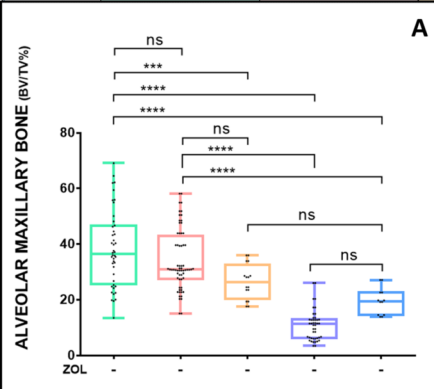
Opg	Rank ^{Tg}	ZOL -				ZOL +					
		SAGITAL	CORONAL	BV/TV % Tb.N (1/mm) Tb.Th (mm)	TMD gr/cm ³	SAGITAL	CORONAL	BV/TV %	Tb.N (1/mm)	Tb.Th (mm)	TMD gr/cm ³
+/+	-			0,0	4,4 ±0,5			17,6±11,5	3,0±1,7	0,1±0,1	4,0±0,3
+/-	-			0,0	4,5±0,4			8,6±6,9	2,8±2,2	0,0	3,8±0,3
+/-	+			0,0	4,4±0,3			69,4±40,7	4,9±1,1	0,1±0,1*	3,6±0,1
-/-	-			0,0	3,5 ±0,3			4,1±3,6	1,5±2,4	0,0	4,0±0,3
-/-	+			0,0	3,7 ±0,6			40,4± 33,2	3,4±3,3	0,0	3,1±0,2

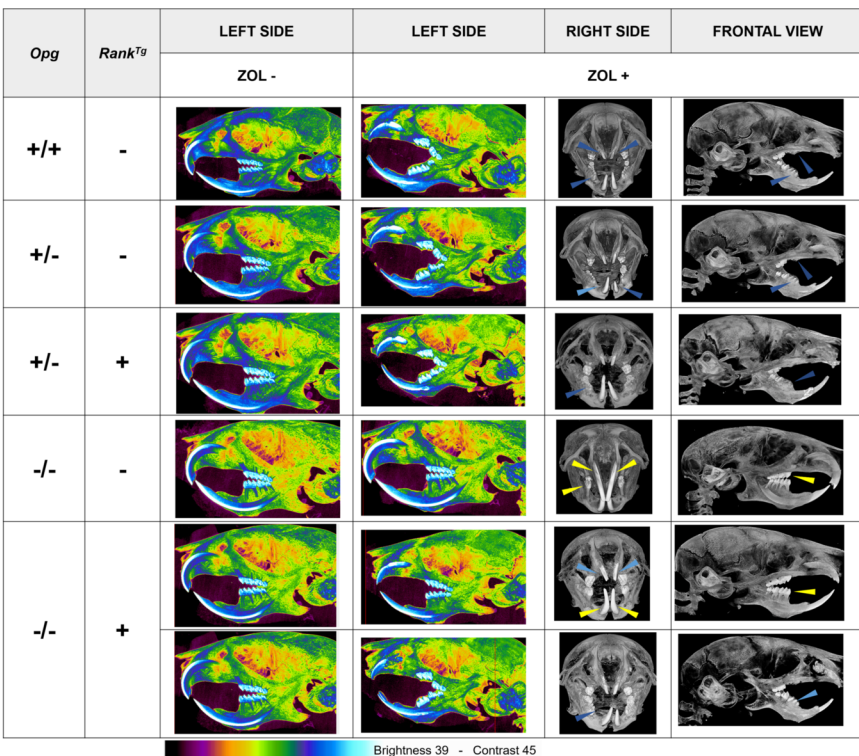
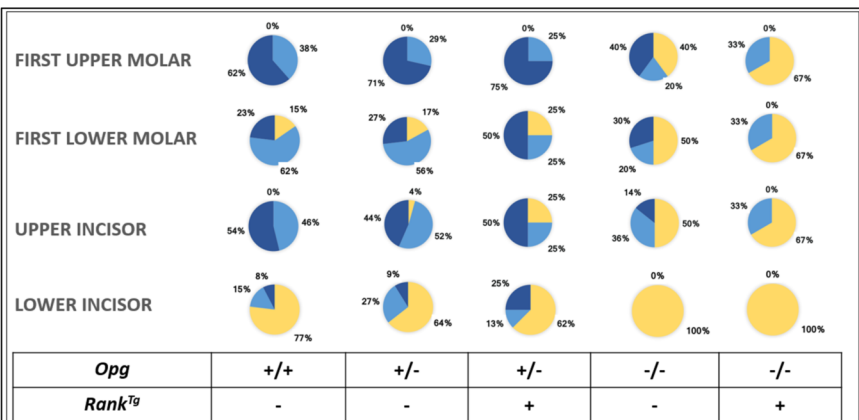
Brightness 39 - Contrast 45

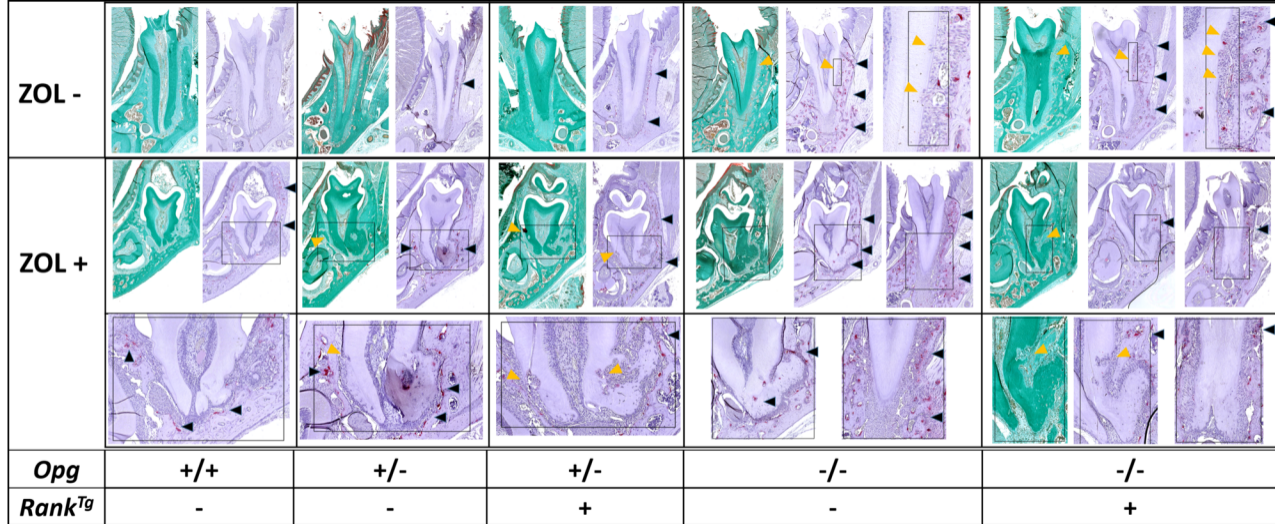
<i>Opg</i>	+/+	+/-	+/-	-/-	-/-
<i>Rank Tg</i>	-	-	+	-	+



	+/+	+/-	+/-	-/-	-/-
<i>Rank</i> ^{Tg}	-	-	+	-	+



A

B


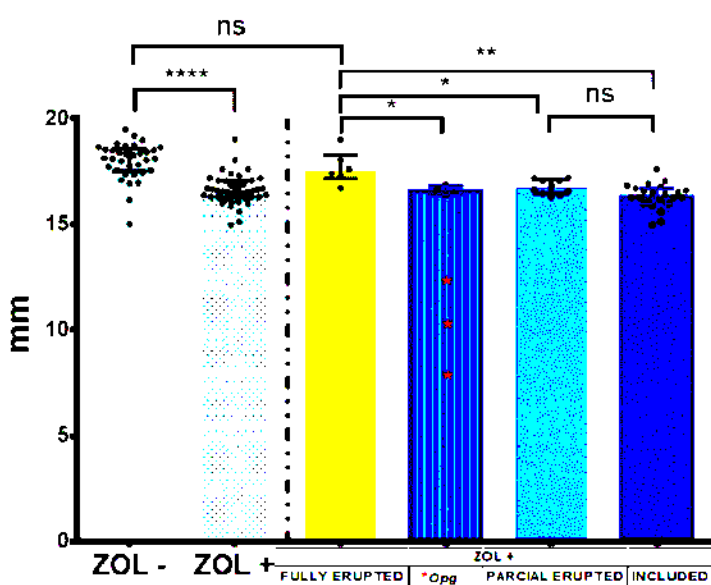


A

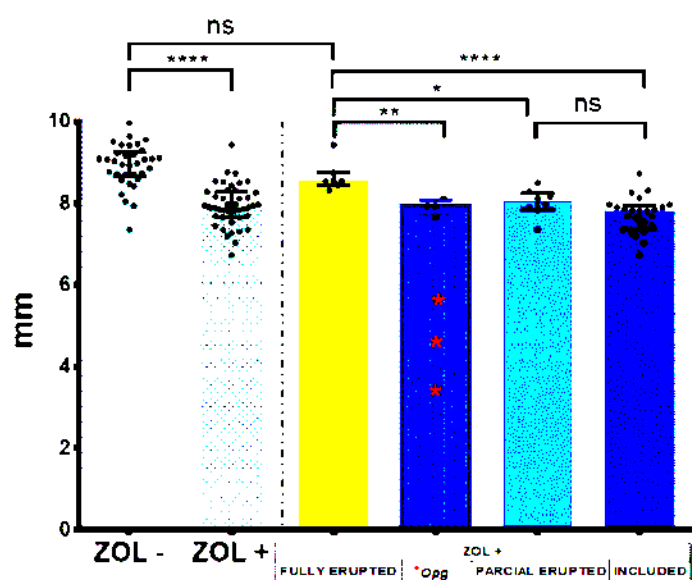
	ZOL +		
<i>Opg</i> ^{+/+} \ <i>Rank</i> ^{Tg-}	0	5	8
<i>Opg</i> ^{+/-} \ <i>Rank</i> ^{Tg-}	0	4	14
<i>Opg</i> ^{+/-} \ <i>Rank</i> ^{Tg+}	0	1	2
<i>Opg</i> ^{-/-} \ <i>Rank</i> ^{Tg-}	4	*1	*2
<i>Opg</i> ^{-/-} \ <i>Rank</i> ^{Tg+}	2	*1	0

B

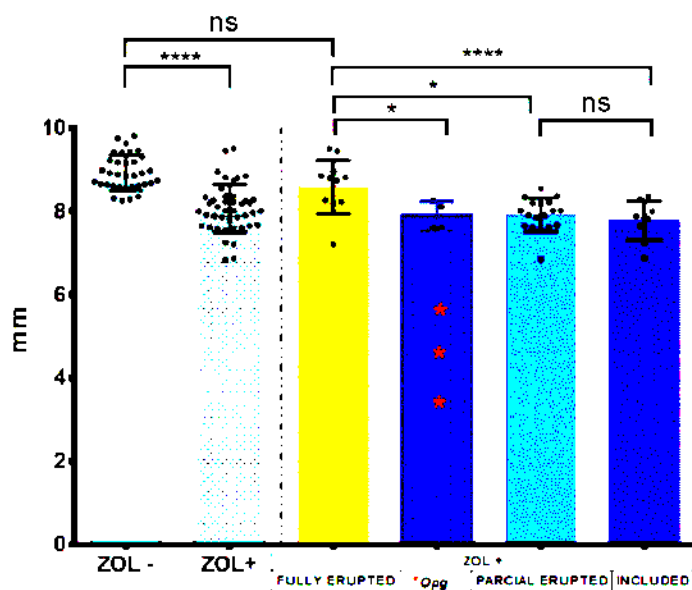
SKULL LENGTH (E) /
UPPER MOLAR ERUPTION

**C**

FACIAL REGION LENGTH (G) /
UPPER UPPER MOLAR ERUPTION

**D**

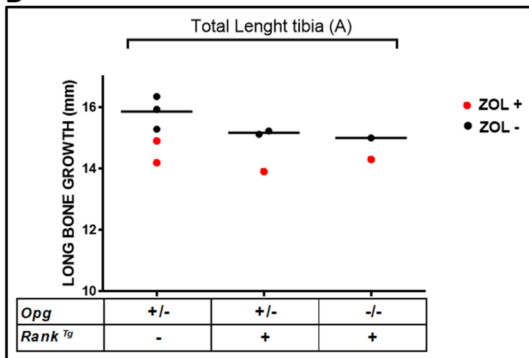
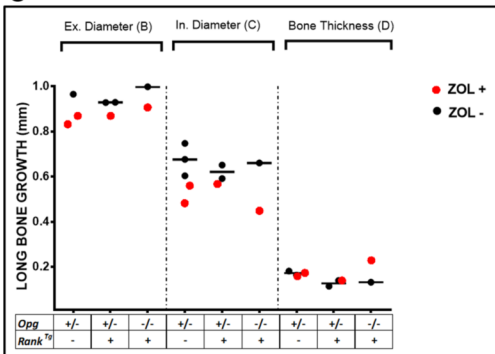
MANDIBULAR LENGTH (J) /
LOWER MOLAR ERUPTION



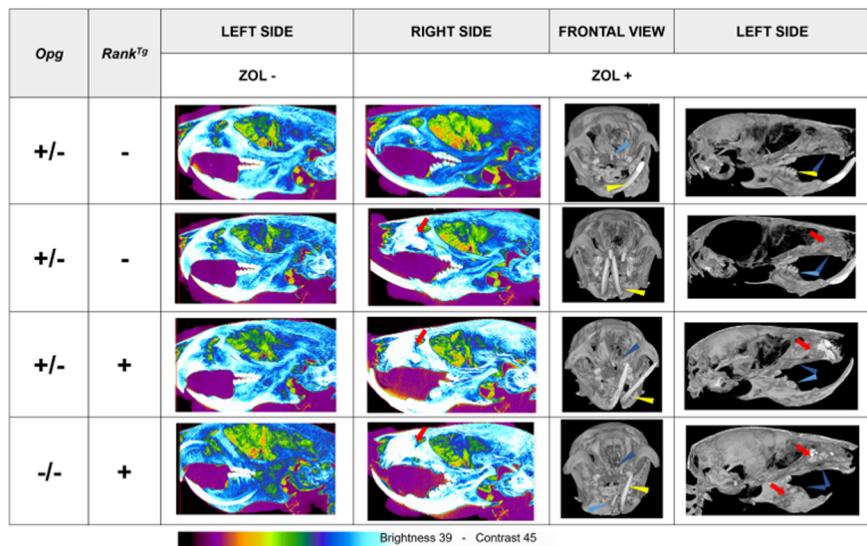
A

ZOL	<i>Opg</i>	<i>Rank^{Tg}</i>	SAGITAL	CORONAL	BV/TV %	Tb.N 1/mm	Tb.Th mm	TMD gr/cm ³
-	+/-	-			0,0	0,0	0,0	4,7
	+/-	-			0,0	0,0	0,0	4,6
	+/-	+			0,0	0,0	0,0	4,7
	-/-	+			0,0	0,0	0,0	3,8
+	+/-	-			4,9	0,6	0,1	5,0
	+/-	-			0,0	0,0	0,0	5,0
	+/-	+			67,9	5,9	0,1	4,1
	-/-	+			24,3	2,8	0,1	5,1

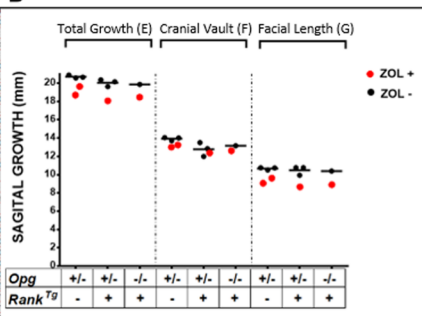
Brightness 39 - Contrast 45

B**C**

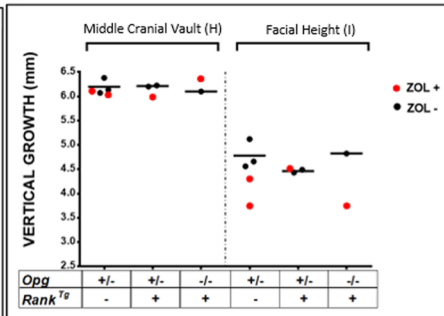
A



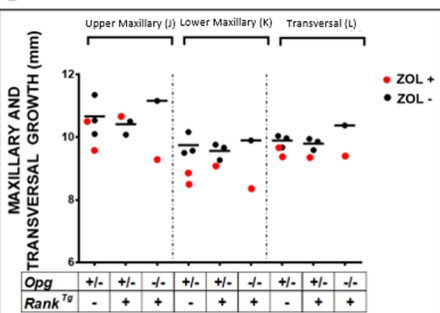
B



C



D



MODEL

PROTOCOL

EUTHANASIA

RESULTS

C57BL/6J
(Six per group)

CONTROL

Opg^{+/+}
Rank^{Tg-}

Opg^{+/-}
Rank^{Tg-}

Opg^{-/-}
Rank^{Tg+}

Opg^{+/+}
Rank^{Tg+}

Opg^{+/-}
Rank^{Tg+}

Opg^{-/-}
Rank^{Tg+}

GENOTYPE CORRESPONDING TO
DIFFERENT RANKL SIGNALING ACTIVITY LEVELS

ZOLEDRONIC ACID

4 injections

50ug/kg

DAY AFTER BIRTH

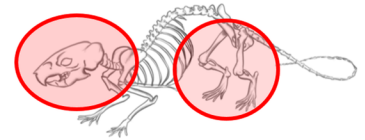


1 ½ MONTH



10 MONTHS

PHENOTYPE OF CRANIOFACIAL AND APPENDICULAR SKELETONS



- Growing arrest.
- Bone density modifications.
- Tooth eruption arrest.
- Incisor neoplasia's-like structure.

PHENOTYPE MODULATIONS COMPARE TO CONTROL

